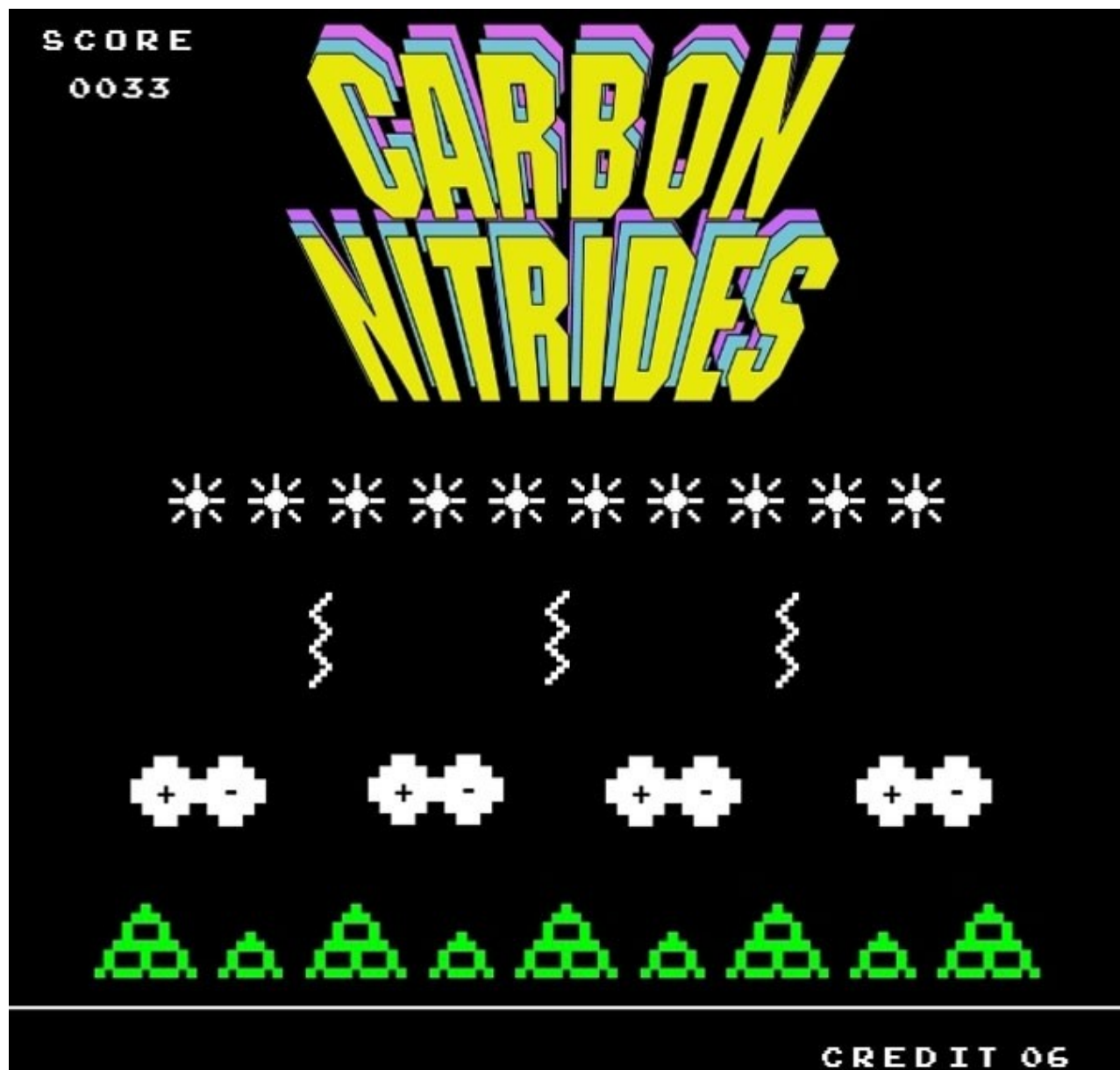


# Emerging Concepts in Carbon Nitride Organic Photocatalysis

Stefano Mazzanti<sup>[b]</sup> and Aleksandr Savateev<sup>\*[a]</sup>



Carbon nitrides encompass a class of transition-metal-free materials possessing numerous advantages such as low cost (few Euros per gram), high chemical stability, broad tunability of redox potentials and optical bandgap, recyclability, and a high absorption coefficient ( $>10^5 \text{ cm}^{-1}$ ), which make them highly attractive for application in photoredox catalysis. In this Review, we classify carbon nitrides based on their unique properties, structure, and redox potentials. We summarize recently emerging concepts in heterogeneous carbon nitride

photocatalysis, with an emphasis on the synthesis of organic compounds: 1) Illumination-Driven Electron Accumulation in Semiconductors and Exploitation (IDEASE); 2) singlet-triplet intersystem crossing in carbon nitride excited states and related energy transfer; 3) architectures of flow photoreactors; and 4) dual metal/carbon nitride photocatalysis. The objective of this Review is to provide a detailed overview regarding innovative research in carbon nitride photocatalysis focusing on these topics.

## 1. Introduction

Electron transfer is a universal method to activate organic molecules that can be triggered, for example, by chemical oxidants/reductants, or employing mechanoredox catalysis,<sup>[1]</sup> electrocatalysis,<sup>[2]</sup> and photoredox catalysis.<sup>[3]</sup> The aforementioned catalytic approaches require a material (the catalyst) to convert a specific type of energy into the driving force for substrate oxidation and reduction. In mechanoredox catalysis – piezoelectric materials and mechanical energy, in electrocatalysis – electrically conductive materials and electric current, in photoredox catalysis – light responsive molecules and photons (electromagnetic radiation) represent the catalyst and energy, respectively. Catalytic redox approaches are more material efficient compared to purely chemical approaches, as they ideally require only energy which can be derived from renewable sources and the catalyst. However, these approaches come with some drawbacks, such as the employment of sacrificial agents, and degradation of electrodes. Nevertheless, Reisner et al. demonstrated that biomass can be employed as a sustainable electron donor in net-reductive reactions.<sup>[4]</sup> On the other hand, purely chemical approach would require employment of toxic or explosive agents, and generates considerable amounts of waste derived from auxiliary agents. Taking into account all these pros and cons catalytic approach appears to be much more appealing.<sup>[5]</sup>

While mechanoredox catalysis is a very recent concept that has not been investigated extensively in preparative organic chemistry, electrocatalysis and photoredox catalysis radically changed the field of catalysis; including how organic chemists conceive the strategies for synthesis or functionalization of a desired molecule.<sup>[6]</sup>

Verschueren and Borggraeve indicated the shared attributes of these approaches,<sup>[7]</sup> but they also possess unique features. For example, a photoredox approach functions better in overall redox neutral reactions, due to the fact that oxidation and reduction steps are executed by the same species, while electrocatalysis offers a greater tolerance to functional groups due to precise control over electrolysis parameters, namely voltage or current. Except few reports, electro- and photocatalysis are employed separately in synthesis of organic molecules,<sup>[6a]</sup> but develops conjunctly, as photoelectrocatalysis in water splitting and CO<sub>2</sub> conversion.<sup>[8]</sup>

Growth of concepts related to the synthesis of organic molecules in the past two decades have benefitted from the large number of tunable parameters accessible in photocatalysis. For example, photocatalyst redox potentials as well as the energy and intensity of incident light utilized for energy transfer in photocatalytic systems,<sup>[9]</sup> multiphoton/chromoselective catalysis,<sup>[10]</sup> and proton coupled multielectron transfer.<sup>[11]</sup>

To properly explore these and other concepts in photocatalysis, we would like to give a brief overview of materials used as photocatalysts, their key features, and advantages.

### 1.1. Overview of photocatalytically active materials


Although, Ir(III) and Ru(II)<sup>[12]</sup> complexes were among the first redox active sensitizers in organic synthesis, their high cost motivated scientists to develop alternatives based on earth-abundant transition metals,<sup>[13]</sup> metal free organic dyes such as flavins,<sup>[14]</sup> and other commercially available compounds.<sup>[15]</sup>

Higher thermal and chemical stability, ease of recovery from the reaction mixture, and recyclability make semiconductor materials more attractive in comparison to molecular systems.<sup>[16]</sup> Processability of semiconductors alongside insolubility within common solvents make them extremely useful for the fabrication of nano-, micro- and macro-structures with applications in photocatalysis as coatings in microfluidic reactors,<sup>[17]</sup> active layers in photoelectrocatalysis,<sup>[18]</sup> photocatalytically active monoliths<sup>[19]</sup> and aerogels.<sup>[20]</sup>

Based on elemental composition, semiconductor materials can be divided into several classes: inorganic materials, represented by metal oxides and chalcogenides,<sup>[21]</sup> as well as perovskites,<sup>[22]</sup> metal organic frameworks, composed of metal linker and organic ligand,<sup>[23,24,25,26]</sup> and organic materials, built exclusively from organogenic elements.

[a] Dr. A. Savateev  
Department of Colloid Chemistry  
Max Planck Institute of Colloids and Interfaces  
Research Campus Golm  
Am Mühlenberg 1, 14476 Potsdam (Germany)  
E-mail: oleksandr.savatieiev@mpikg.mpg.de

[b] S. Mazzanti  
Department of Colloid Chemistry  
Max Planck Institute of Colloids and Interfaces  
Research Campus Golm  
Am Mühlenberg 1, 14476 Potsdam (Germany)

 © 2020 The Authors. ChemPlusChem published by Wiley-VCH GmbH. This is an open access article under the terms of the Creative Commons Attribution License, which permits use, distribution and reproduction in any medium, provided the original work is properly cited.

Although unitary metal oxides, such as  $\text{TiO}_2$ ,<sup>[27]</sup> have been one of the mainly used photoactive materials since 1970, binary and ternary metal oxides hold promise in photocatalytic applications. Primarily, this is due to precise tuning of the optical band gap as it has been shown by Le Bahers and Takanabe, and higher efficiency, as demonstrated by Kudo's group.<sup>[28]</sup> Furthermore, Marschall et al. synthesized a series of pyrochlores (compounds with general formula  $\text{A}_2\text{M}_2\text{O}_6\text{X}$ , in which A and M are cations and X is the counter ion) featuring enhanced absorption up to near IR due to the presence of defects,<sup>[29]</sup> while  $\text{CaFe}_2\text{O}_4$  with a hierarchical pore morphology and spinel ferrites  $\text{ZnFe}_2\text{O}_4$  and  $\text{MgFe}_2\text{O}_4$  were used for the fabrication of photoelectrodes.<sup>[30]</sup> Mixed metal oxides have additionally been employed in different photocatalytic devices, including large scale solar-driven redox photovoltaic-electrochemical systems.<sup>[31]</sup> Overall, the field of metal oxide photocatalysis is very rich, but detailed analysis is beyond the scope of this review. Therefore, we refer to the reviews authored by the experts in this area of research.<sup>[32]</sup>

Purely organic semiconductors differentiate themselves from inorganic materials in terms of improved ability for design.<sup>[33]</sup> Indeed, even when taking into account only commercially available building blocks, there is an overwhelming amount of materials, with specific structures adjusted for a specific application.<sup>[34]</sup> Related to organic photoredox catalysis, in a series of works Zhang et al. used covalent triazine frameworks in the synthesis of benzophosphole oxides,<sup>[35]</sup> porous poly-benzobisthiadiazole network in the dehalogenation reaction of  $\alpha$ -bromoacetophenones,<sup>[36]</sup> donor-acceptor COFs in coupling of heteroarenes with diethyl bromomalonate,<sup>[37]</sup> and poly(benzothiadiazole) in [2 + 2] cycloaddition of styrene.<sup>[38]</sup> Benzo-thiadiazole-based microporous organic polymers were also used in bromination of electron rich aromatic compounds,<sup>[39]</sup> and poly-benzobis-thiadiazoles in the synthesis of fused 1,2,3,4-tetrahydroquinolines respectively,<sup>[40]</sup> while in-depth mechanistic studies revealed the formation of singlet oxygen ( $^1\text{O}_2$ ) in these reactions which univocally confirmed the energy transfer path. Detailed summary of COFs synthesis and application in organic photoredox catalysis is given in the reviews.<sup>[41]</sup>

Carbon nitrides (CNs) stand out from transition metal free heterogeneous photocatalysts due to the alternating C–N bonds in their structure. CNs are a family of materials, composed of polymeric chains and graphitic layers of N-rich aromatic rings, with monomeric units constituted by triazine or heptazine units linked together by N bonds ( $\text{sp}^3$ ), with an ideal

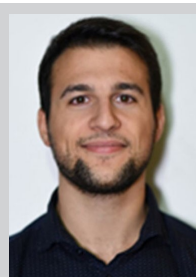
ratio in graphitic carbon nitride structure of 3:4 C/N.<sup>[42]</sup> They are prepared by the calcination of N-rich compounds, such as urea and melamine, producing architectures which absorb light in the visible range.

Over years of research, different approaches for CNs preparation have emerged. Thus, Shalom et al. introduced a concept of supramolecular preorganization of monomers, such as cyanuric acid and melamine.<sup>[43]</sup> This approach was later employed in the synthesis of CN of different morphologies, such as micron-sized CN tubes for dye degradation,<sup>[44]</sup> micron-sized sheets for dye adsorption and degradation,<sup>[45]</sup> continuous 500 nm–10  $\mu\text{m}$  thick CN films for photoelectrochemistry (PEC),<sup>[46]</sup> hierarchically structured nanoporous CN with edelweiss-like morphology,<sup>[47]</sup> and 1D nanofibers for  $\text{O}_2$  liberation from water.<sup>[48]</sup> Comprehensive summary of supramolecular approach in CNs synthesis can be found in the review.<sup>[49]</sup>

Apart from supramolecular preorganization of monomers, several methods such as using appropriate starting precursors,<sup>[50]</sup> template,<sup>[51]</sup> pre- or post-treatment,<sup>[52]</sup> metal- or nonmetal- and molecular doping<sup>[53]</sup> are commonly employed to adjust CNs properties. The following paragraphs highlight some of these strategies in greater detail.

Although, melamine and urea are the cheapest commercial precursors for CNs preparation, using more complex but easily accessible molecules, such as 3-amino-1,2,4-triazole oligomer,<sup>[54]</sup> can be beneficial to transfer morphology of the precursor to the final CN via the 'topotactic-like' phase transition as has been shown by Dontsova et al.<sup>[55]</sup>

Templating is a commonly used method to increase surface area of carbon nitrides and, in general, an indispensable tool in materials chemistry. The development of porous carbon nitrides is essential to overcome restrictions related to low surface area, and suppress charge recombination for application in heterogeneous photocatalysis.<sup>[56]</sup> Vinu et al. synthesized a class of CN materials with different carbon-to-nitrogen ratios. In this manner optoelectronic and physicochemical properties of CN materials can be modulated for different applications.<sup>[56a,57]</sup> Thus,  $\text{C}_3\text{N}_5$  material have been prepared by self condensation of 3-amino-1,2,4-triazole inside confined mesopores of KIT-6 silica at 500 °C. Higher nitrogen content resulted in enhanced rate of  $\text{H}_2$  production due highly ordered 3D structure with a high surface area, reduced band-gap with improved absorption in the visible solar spectrum, and by capturing more photons due to a light scattering effect inside the pores. Even more nitrogen enriched materials, i.e.  $\text{C}_3\text{N}_6$ , were synthesized by the same group with a similar template method, employing amino-



Stefano Mazzanti received his M.Sc. degree in Industrial Chemistry at the University of Bologna. Since 2019 he started his PhD at the Max Planck Institute of Colloids and Interfaces, with Aleksandr Savateev as mentor and Markus Antonietti as supervisor. His research is focused in the development of novel photocatalytic processes mediated by carbon nitride photocatalysts.



Aleksandr Savateev received his PhD degree in Organic Chemistry in 2016 and shortly after that he started his research group 'Innovative Heterogeneous Photocatalysis' at the Max Planck Institute of Colloids and Interfaces in Potsdam, Germany. His research interests stand on the border between physical chemistry, solid state chemistry, photochemistry and catalysis, but applied mainly to synthesis of organic molecules.

guanidine hydrochloride as the precursor, which also displayed higher activity toward  $H_2$  production compared to carbon nitride with the  $C_3N_4$  stoichiometry. The field is still expanding toward materials with a higher C/N ratio, such as  $C_3N_7$ , finding application in electrochemical oxygen reduction.<sup>[58]</sup>

Heteroatom doping is a reliable method to introduce different elements into the CN backbone, effectively changing electrical, optical and morphological properties of the material. Heating trithiocyanuric acid at 650 °C was reported to yield sulfur doped CN. The photocatalyst prepared via this straightforward approach presented 12 times higher activity in hydrogen evolution reaction (HER) and 5 times higher activity in oxygen evolution reaction (OER). Doping of CN with sulfur also allowed the material to perform OER without the employment of any metallic co-catalyst.<sup>[53d]</sup>

Boron carbon nitride can be prepared from boron oxide and melamine in bulk at 650 °C, achieving better photodegradation of Rhodamine B, compared to undoped material.<sup>[50b]</sup>

Other nonmetal atoms, such as halides, may be employed in heteroatom doping of CNs. Iodine doped carbon nitride can be obtained by heating dicyanamide with ammonium iodine at 550 °C. This doping extends the UV-vis absorption spectrum up to 600 nm compared to g-CN, and doubles  $H_2$  production rates.<sup>[53c]</sup> Beyond the edges of photocatalysis, mesoporous CNs doped with sulfur and phosphorus also found application in energy storage.<sup>[59]</sup>

Zhang and Wang employed different approaches to tune CNs properties by introducing electron deficient monomers into the CN structure to enhance photocatalyst performance in HER,<sup>[60]</sup> constructing internal triazine-heptazine donor-acceptor (D-A) heterostructure to reach AQY 60% in HER,<sup>[61]</sup> using elemental doping with selenium for bioapplications.<sup>[62]</sup>

Finally, a heterojunction between two or more semiconductors is used to improve performance of the hybrid material by reducing the recombination rate of photogenerated charge carriers. For example, Yu and Zhang developed a 0D/2D S-Scheme heterojunction material composed of  $CeO_2$  quantum dots and CN for photocatalytic deactivation of bacteria.<sup>[63]</sup> Zou and Shi designed a complex  $Zn_xCd_{1-x}In_2S_4$  solid solution coupled with CN nanosheets as a 2D/2D heterostructure,<sup>[64]</sup> a material possessing heterojunction between CdS,  $WO_3$  and CN,<sup>[65]</sup> and ultrathin CN nanosheets modified with  $Cu_2MoS_4$  for  $H_2$  liberation.<sup>[66]</sup>

Overall, a comprehensive summary on CNs synthesis, characterization, properties, and environmental applications are available in reviews.<sup>[67]</sup> At the same time, application of carbon nitrides in organic photoredox catalysis has been summarized in the dedicated reviews.<sup>[68,69,70,71]</sup>

Recapitulating available literature we conclude that, in general, CN-based photocatalysts of sophisticated structure, such as those featuring heterojunction and exquisite morphology, are employed in water splitting and environmental applications (model reactions), while CNs photocatalysts with large surface area and stoichiometry close to  $C_3N_4$  are commonly employed in organic synthesis.

It should be noted that although quasi monochromatic artificial light generated by cost effective LEDs is typically

utilized in organic photoredox catalysis, several works report using solar light under outdoor conditions in CN mediated organic synthesis that illustrates solar-to-chemicals concept in sustainable transition metal free heterogeneous organic synthesis.<sup>[72]</sup>

The interesting concept of using a combination of CNs and electron mediator,  $O_2$  or methyl viologen, as 'light-activated acid' in organocatalysis has been validated in synthesis of ketals and acetals, a reaction that typically requires acid catalysis.<sup>[73]</sup>

Finally, we would like to point out that the application of carbon nitrides in light energy conversion extends beyond organic synthesis. They are also used as a radical photoinitiator,<sup>[74]</sup> in construction of photo-electrochemical and electrochemical devices,<sup>[75]</sup> sensors, photonics, and hydrogels.<sup>[76]</sup>

Remarkable progress in the field of CN-based photocatalysis clearly demonstrates the ever-growing interest of the scientific community in this class of materials. Therefore, we believe, it is an opportune moment to summarize emerging concepts in carbon nitride organic photocatalysis.

In this review, focused on organic chemistry readership, we classify CN materials into ionic and covalent structures based on chosen preparation methods and their properties. Thereafter, emerging fields, namely the application of CN materials and their long-lived radicals in energy transfer, flow chemistry, and metal/dual photoredox catalysis, are explored in a concept-wise approach. Therefore, the objective of this review is to ease the development of new processes and to help facilitate interdisciplinary research centered around CN materials. Indeed, despite the exponential growth of publications concerning CN, only few works are related to aforementioned topics and there are no reviews discussing them in a comprehensive manner. Furthermore, to account for the abundant works related to the chemistry of carbon nitride material design and application which are beyond the scope of this review, we refer to specialized papers authored by experts in their respective field in the subsequent paragraphs.

## 1.2. General mechanism in molecular and semiconductor photocatalysis

To give a better description of carbon nitride photocatalysis, in this paragraph we compare the differences and similarities between a general mechanism used in molecular photoredox catalysis with semiconductor photocatalysis. An in-depth understanding of the mechanism guarantees exploration of new reaction pathways in organic synthesis, and avoids the pitfalls of data interpretation.

Photoredox catalysis enables selective generation of open-shell species via a sequence of processes summarized in Figure 1.<sup>[77]</sup> This process starts with the excitation of the photocatalyst (PC), from the ground state to the excited state (PC\*). Here, an electron is promoted to the LUMO, creating a vacancy in the HOMO thus giving rise to a more active redox agent. Afterward, in the presence of substrates with suitable redox properties, the photocatalyst undergoes photoinduced electron transfer (PET), a process generally exploited to

## Photoinduced electron transfer pathways

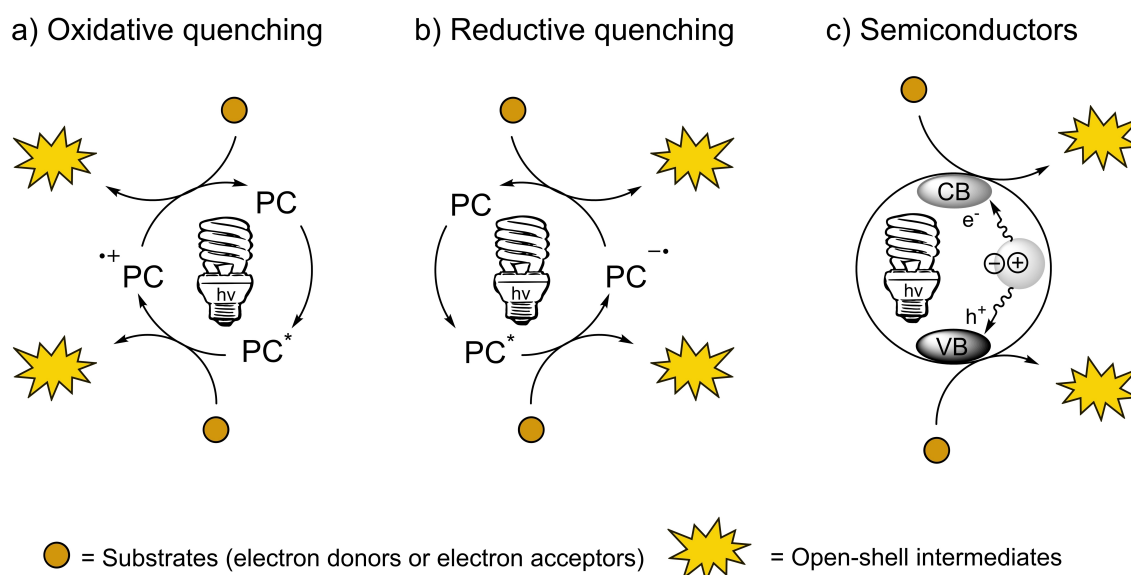


Figure 1. Photoredox mechanism comparing molecular photocatalysts and semiconductors.

generate open-shell species.<sup>[78]</sup> In all elementary steps shown in Figure 1, the substrate is either a synthetically useful organic molecule or sacrificial electron donor/acceptor. If a photocatalytic reaction requires sacrificial electron donors, such as amines or alcohols, the process is defined as 'net reductive'. If electron acceptors, for example,  $O_2$ ,  $PhNO_2$  or  $(NH_4)_2S_2O_8$ , the reaction is 'net oxidative'. If no sacrificial agent is added, the process is 'net redox-neutral'.<sup>[79]</sup>

When the excited state of the photocatalyst is oxidized (formation of  $PC^{*+}$ ) by the substrate or sacrificial electron acceptor, (and turnover is completed by oxidation of the sacrificial electron donor or another substrate), the pathway is called oxidative quenching (Figure 1a).

Oxidative quenching is operative, for example, with phenanthrene,<sup>[80]</sup> 9-mesityl-10-methylacridinium perchlorate (Mes-Acr-Me),<sup>[81]</sup> eosin Y,<sup>[82]</sup> and  $Ir(dF(CF_3)ppy)_2(dtbbpy)PF_6$  in the corresponding chemical transformations.<sup>[83]</sup>

On the other hand, if the catalyst is first reduced (formation of  $PC^{*-}$ ) by the substrate, or sacrificial electron donor (and turnover is then completed by reduction of another substrate or electron acceptor), the pathway is called reductive quenching (Figure 1b).<sup>[84]</sup> Reductive quenching has been reported, for example, for 1,4-dicyanonaphthalene (DCN),<sup>[85]</sup> 9,10-dicyanoanthracene (DCA),<sup>[86]</sup> 2,4,6-tri(*p*-tolyl)pyrylium tetrafluoroborate (*p*-Me-TPT),<sup>[87]</sup> 3-cyano-1-methylquinolinium perchlorate ( $QuCN^+ ClO_4^-$ ),<sup>[88]</sup> 9-mesityl-10-methylacridinium perchlorate (Mes-Acr-Me),<sup>[89]</sup> eosin Y and  $Ru(bpy)_3^{2+}$ .<sup>[84,90]</sup>

Overall, the redox properties of the photocatalyst with respect to the redox properties of the substrates define whether oxidative or reductive quenching takes place in the specific reaction. Nevertheless, in both pathways substrates are con-

verted to radical ions, which are more reactive compared to their neutral precursors.

In semiconductor photocatalysis, the terms valence band (VB) and conduction band (CB) are used to denote 'sites' on the energy scale for substrate oxidation and reduction, respectively. The bands edges, VB maximum and CB minimum, can be considered as equivalents of HOMO and LUMO. When an incident photon interacts with the surface exciton, it splits into a hole and electron, establishing charge separation between VB and CB. Unlike to molecular photocatalysis that considers formation of  $PC^{*-}$  and  $PC^{*+}$  and, therefore, implies stepwise mechanism, in semiconductor photocatalysis PET, substrate oxidation and reduction, occur simultaneously (Figure 1c). In Section 2, however, we provide an example in which the mechanism of carbon nitride excited state reductive quenching is operative.

### 1.3. Synthesis and structure of carbon nitride materials

Chemical composition, morphology, and properties of CNs depend on the synthetic approach. Indeed, material engineering is a key step to tune the material toward specific applications. The great ensemble of materials with a general name of carbon nitrides can be divided into two categories: covalent and ionic CNs (Figure 2).<sup>[69,91]</sup>

The crucial difference is that covalent CNs do not have ionic N bonds – they possess only covalent C–N bonds or contain equal amount of cations and anions that are delocalized and intercalated between the  $\pi$ -conjugated layers and N–H functionality.<sup>[92]</sup> On the other hand, ionic CNs have negatively charge N atoms, bonded with metal cations.<sup>[93]</sup> Powder X-ray

## Covalent Carbon Nitrides

## Ionic Carbon Nitrides

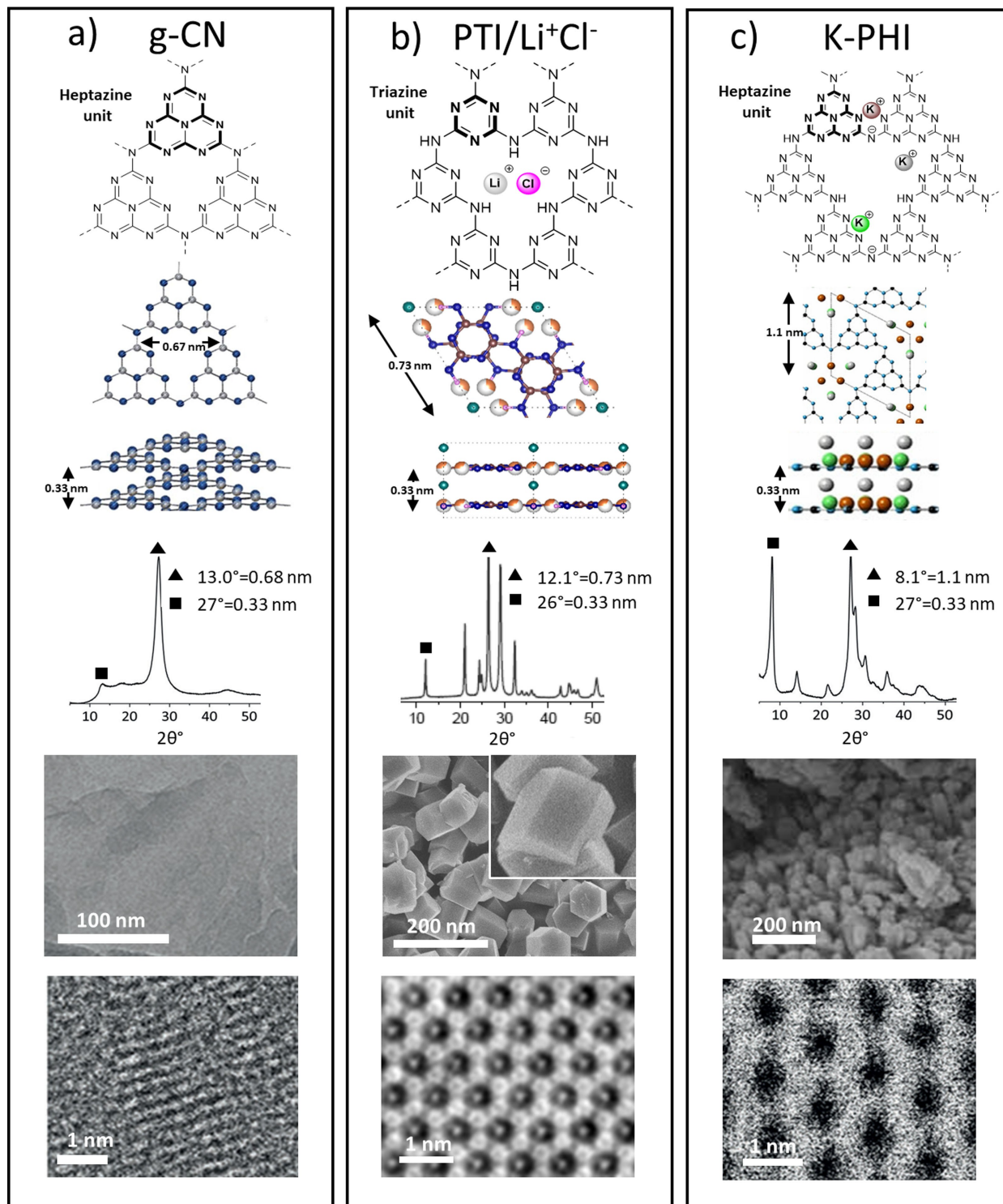


**Figure 2.** Carbon nitride model materials. Following in vertical order: structure representation, PXRD, SEM, and TEM. a) g-CN. Reproduced and modified from reference [53 m, 71] with permission from The Royal Society of Chemistry and Wiley-VCH, respectively. b) PTI/Li<sup>+</sup>Cl<sup>-</sup>. c) K-PHI. Reproduced and modified from reference [71, 99b] with permission from Wiley-VCH.

diffraction (PXRD), scanning electron microscopy (SEM), and transmission electron microscopy (TEM) can be considered as

the fingerprints to identify the type of synthesized CN (Figure 2).

In this review, graphitic CN (g-CN),<sup>[73b,91,94]</sup> mesoporous graphitic CN (mpg-CN),<sup>[95]</sup> and poly(triazine imide) intercalated with LiCl (PTI/Li<sup>+</sup>Cl<sup>-</sup>),<sup>[96]</sup> represent covalent CNs. Preparation of paterfamilias g-CN is the most straightforward – melamine, or analogous precursors, is simply calcinated at 550–600 °C to obtain a metal free polymeric semiconductor. In PXRD, g-CN is characterized by peaks at 13° and 27°, due to in-plane periodicity formed by tri-substituted heptazine units and inter-layer stacking similar to that in graphite, respectively (Figure 2a). g-CN is a mainly amorphous material, as typically seen from SEM and TEM images. Higher intensity of the diffraction peak at 27° indicates a preference of g-CN to form layered structure due to  $\pi$ - $\pi$  stacking, which can be verified in TEM image (Figure 2a) as a stack of 5–10 layers. At the same time, relatively low intensity of the diffraction peak at 13° indicates relatively few repeating units in the plane.

mpg-CN has a similar chemical structure to the graphitic predecessor, but has greater catalytic activity due to larger surface area,  $> 200 \text{ m}^2 \text{ g}^{-1}$ .<sup>[97]</sup> Preparation of mpg-CN belongs to the hard template synthesis method, which employs cyanamide as the precursor, and colloidal silica aqueous solution, followed by calcination at 550 °C and washing with ammonium bifluoride for template removal.<sup>[95d]</sup>

PTI/Li<sup>+</sup>Cl<sup>-</sup> is a more crystalline member of covalent CNs (Figure 2b). It is composed of tri-substituted triazine units and can be prepared by calcining dicyanamide in a LiCl/KCl eutectic salt mixture at 400–600 °C.<sup>[96h]</sup> In this case, the eutectic salt mixture serves as a template and directs precursor polymerization toward PTI/Li<sup>+</sup>Cl<sup>-</sup> instead of g-CN. PXRD pattern of this material shows many intense peaks, whereby 12.1° and 26° have been assigned to in-plane periodicity and layers stacking respectively, which were also confirmed by high resolution TEM.<sup>[96a,h]</sup> SEM images show beautiful crystallites of tridimensional hexagonal shape with diameter  $\sim 1 \mu\text{m}$ . Structure is further confirmed by aberration-corrected integrated differential phase contrast TEM (AC-IDPC TEM) imaging, showing the interconnected triazine pattern. Even though PTI/Li<sup>+</sup>Cl<sup>-</sup> shows highly geometrical and beautiful structure, its application at this moment is limited to HER only. Nevertheless, due to its highly organized structure, PTI/Li<sup>+</sup>Cl<sup>-</sup> offers an excellent platform to study reactivity of different facets in photocatalysis as has been demonstrated by Lin and Wang.<sup>[96a]</sup>

In the other category, ionic CNs are constituted by poly (heptazine imide)s (PHIs) and cyanamide surface-functionalized melon-type carbon nitride ( $^{\text{N}}\text{CN}_x$ ).<sup>[98]</sup> Heptazine units are the building blocks in these materials. Potassium PHI (K-PHI) has been selected as a model material because of its broadly documented application in organic synthesis, and in depth characterization (Figure 2c).<sup>[69,98–99]</sup> The structure is highly ordered compared to g-CN, although still possessing a large amount of structural defects such as unit cell distortions, faults in the sequences of CN-layer stacking, edge and screw dislocations as well as rippling of CN-layers.<sup>[99b]</sup> The ordered motifs of K-PHI are constructed from six heptazine units observed as a honeycomb structure in TEM images. In PXRD, K-PHI can be easily recognized by the appearance of a diffraction peak at 8°. The peak at 27°, attributed to layer stacking that is a

common feature for all types of CNs, and in general for graphite-like materials, is also observed in the K-PHI PXRD pattern. From SEM images, it appears as nanospherulites with diameter in the range of 30 to 300 nm.

For K-PHI, three main preparation methods have been reported: 1) mechanochemical pretreatment of 5-aminotetrazole in LiCl/KCl eutectic mixture followed by calcination at 550 °C,<sup>[100]</sup> 2) from dicyanamide, KSCN and potassium melonate penta-hydrated calcinated at 500 °C or from trichloromelamine,<sup>[99]</sup> 3) KSCN and LiCl calcinated at 550 °C.<sup>[101]</sup> At the same time, alkali metal poly (heptazine imide)s (M-PHIs) are prepared via an ionothermal approach employing Na, K and Cs based salts.<sup>[100]</sup> Such cations compensate for negative charges of deprotonated amino functionalities, mediating the interaction between different layers and giving rise to a more ordered structure. Once PHIs are synthesized, they can undergo cation exchange and, if treated with HCl, are converted into H-PHI, or covalent CN, in the notation of this review. Vice versa, treating H-PHI, or CN oligomeric precursors with alkali metal sources is another approach for PHIs preparation.<sup>[93,98,99d,o,102]</sup>

It should be noted that modification of synthesis conditions of the discussed herein classes of carbon nitride materials have tremendous impact on material fingerprints such as PXRD pattern (diffraction peak position and relative intensity), or morphology observed by SEM and TEM. Indeed, there is a continuum of materials with the stoichiometry close to  $\text{C}_3\text{N}_4$ . Therefore, to assign a proper chemical structure to the CN material, it is essential to consider structural features derived from physical methods, such as PXRD, TEM, solid state NMR, X-Ray photoelectron spectroscopy, together with a materials chemical properties, such as ability to store electrons under light irradiation (discussed below) and ion exchange.

#### 1.4. Optical and photoredox properties

In general, g-CN absorbs light with  $\lambda \leq 460 \text{ nm}$  that gives optical band gap of 2.7 eV (Figure 3a), while the absorption coefficient exceeds  $10^5 \text{ cm}^{-1}$ .<sup>[76a]</sup> However, by selecting an appropriate preparation method, the absorption edge can be shifted up to near IR, while the optical band gap narrows to 1.5 eV.<sup>[55,103]</sup> The g-CN emission maximum is located at 470 nm (figure 3b). K-PHI optical band gap is similar to g-CN, but features extended absorption up to 750 nm, attributed to the presence of intra-band states (Figure 3a).<sup>[99b]</sup> K-PHI emission is observed at 500 nm (Figure 3b). g-CN has VB located at +1.82 V and CB at  $-0.88 \text{ V}$  vs. RHE while VB potential in K-PHI is shifted to +2.54 V and CB to  $-0.09 \text{ V}$  vs. RHE (Figure 3c).

Depending on the preparation method, PTI/Li<sup>+</sup>Cl<sup>-</sup> have a band gap of 2.8–3.2 eV,<sup>[96a,c,e,f]</sup> while the position of VB and CB have not yet been determined.<sup>[104]</sup>

Although steady state absorption and fluorescence spectroscopy can provide basic information related to CNs optical properties, advanced spectroscopic analysis are required to obtain a more comprehensive picture. Transient absorption (TA) and transient photoluminescence (TRPL) are indeed useful tools for this purpose.<sup>[105]</sup> With these techniques, Merschjann and co-

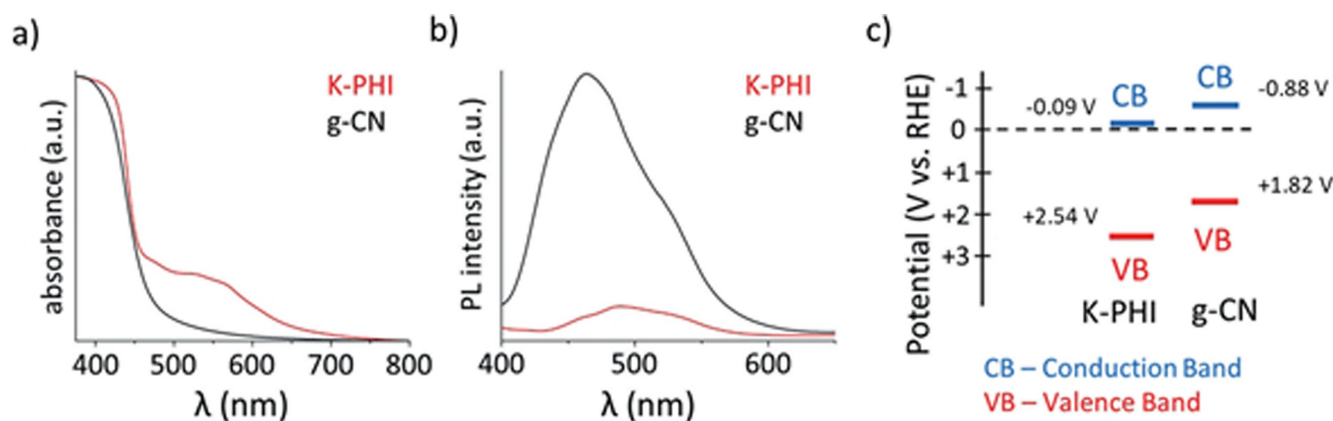


**Figure 3.** Optical properties of g-CN and K-PHI. a) DRUV-vis spectra. b) Photoluminescence spectra. c) VB and CB. Reproduced and modified from reference [71] with permission from Wiley-VCH.

workers analyzed different CN samples.<sup>[106]</sup> They concluded that electrons are transported predominantly perpendicular to graphitic sheets, which is in clear contrast to conductivity in graphene and related materials. From this perspective, AAA stacking of carbon nitride layers is beneficial for electronic transport.<sup>[99b]</sup> These findings led to the conclusion that surface area in heterogeneous carbon nitride photocatalysis correlates rarely with the material photocatalytic activity. Another important conclusion is that nanostructure of CNs, in particular number of layers in *c*-direction, defines material photocatalytic activity. Indeed, based on TRPL data, Zhang et al. concluded that decreasing layer distance in CNs promotes higher electronic transport that leads to higher catalytic activity.<sup>[102]</sup> Furthermore, with these techniques, Durrant et al. showed that CN materials can accumulate long-lived electrons in deep traps that are not reactive in HER.<sup>[107]</sup> Using the spectroscopic study and photocatalytic activity data in HER, they concluded that CNs prepared at lower temperature possess a larger number of  $\text{NH}_2$ -groups, which act as trapping states and decrease activity in HER.

Overall, TA and TRPL are powerful spectroscopic techniques, which give valuable insights into understanding the influence of CNs structural parameters on catalytic activity.

## 2. Illumination-Driven Electron Accumulation in Semiconductors and Exploitation (IDEASE)

In semiconductor photocatalysis, the reaction mechanism implies simultaneous reduction and oxidation of the substrates by photogenerated electrons and holes (Figure 1c). In other words, PET and photocatalyst turnover steps are merged in one synchronous process. This general mechanism has been successfully adopted for covalent CN photocatalysis. However, deviation from this classical mechanism becomes particularly evident, when ionic carbon nitrides are employed in net reductive processes. While covalent CNs participate in photocatalytic transformations via the mechanism proposed by Kisch and depicted in Figure 1c,<sup>[108]</sup> PHIs (in particular K-PHI) behave quite differently, due to the aforementioned structural and morphological features, namely the negatively charged polymeric scaffold and arrangement of heptazine units in a honeycomb-like structure. PHIs change color from yellow to green-blue in the presence of electron donors under light irradiation. Reaction mixture staining, as shown in Figure 4a, is a clear sign of long-lived radical accumulation on the surface and in the bulk of the material (Figure 4a). Steady state absorption spectroscopy shows the rise of an absorption band around

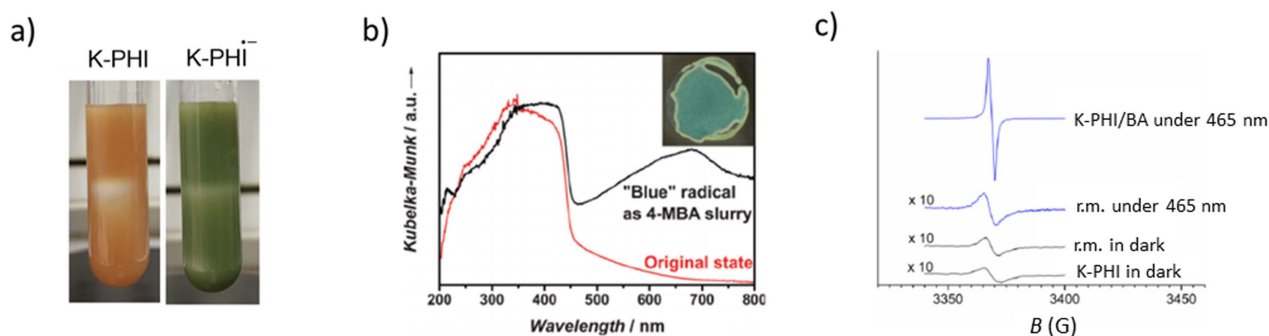


**Figure 4.** Carbon nitride radical anion. a) K-PHI before (left) and after light irradiation (right). Reproduced and modified from reference [99a] with permission from Springer Nature b) Absorption spectra of long-lived radical in  $\text{NCN-CN}_2^-$ . Reproduced and modified from reference [99n] with permission from Wiley-VCH. c) EPR spectra of K-PHI radical anion. Reproduced and modified from reference [99d] with permission from Elsevier.



600–700 nm, as the result of such drastic color change (Figure 4b).

In the EPR spectrum, a sharp uncoupled peak, as a singlet, can be observed as proof of radical formation (Figure 4c).

In-depth EPR studies have shown that there are different kinds of paramagnetic species.<sup>[99b,d,101]</sup> Indeed, they can be attributed to unpaired electrons centered at carbon atoms within the aromatic ring and to ammoniated electrons.<sup>[53i,109]</sup> Spectra from continuous wave EPR also showed anisotropic strains indicating the presence of several types of radicals which differ slightly in their electronic structure. Furthermore, DFT simulation of hyperfine coupling between unpaired electrons, resulted in about 0.7% spin density on the s orbital and about 10% spin density on the p orbital of the <sup>14</sup>N nucleus, which in turn indicates spin localization at one heptazine repeat unit with slight delocalization at the neighboring heptazine units. This data is also in agreement with the work by Markushyna and co-workers, in which it was found that every 4<sup>th</sup> heptazine unit stores one electron,<sup>[99g]</sup> as further proof of charge delocalization to the neighboring units.

Figure 5a compares capacity of different carbon nitride materials – amount of electrons, in  $\mu\text{mol}$ , stored in 1 g of the material. Thus, capacity of ionic carbon nitrides, such as PHIs, is 20 times higher than that of mpg-CN. In this way, when discussing the mechanism of net reductive photocatalytic

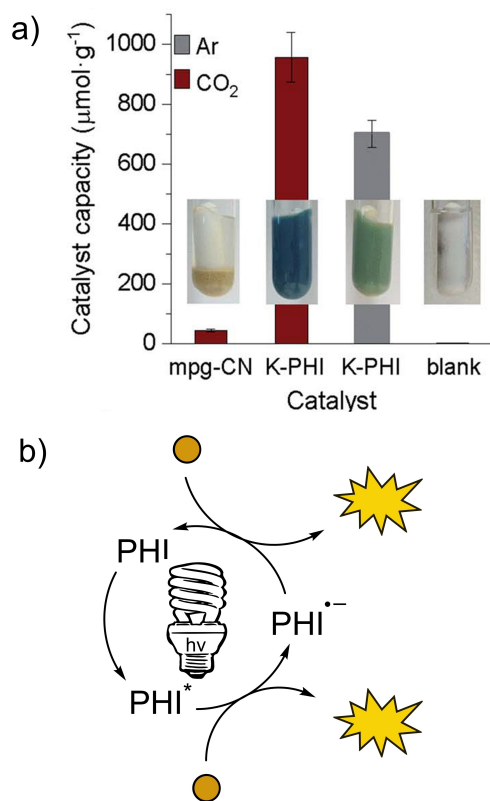


**Figure 5.** Display of PHIs unique feature to form long-lived radical. a) Capacity of covalent (mpg-CN) ionic (K-PHI) carbon nitrides under Ar and CO<sub>2</sub>. Capacity is expressed as the amount of electrons that can be stored in the material ( $\mu\text{mol}(\text{e}^-)\text{g}^{-1}$ ). Reproduced and modified from reference [99 g] with permission from The Royal Society of Chemistry. b) Reductive quenching mechanism of PHI excited state.

reaction mediated by PHIs, reductive quenching is obviously operative as depicted in Figure 5b.<sup>[79]</sup> In this view, behavior of K-PHI and related CN-based materials is similar to homogeneous photoredox catalysis rather than inorganic semiconductors, such as TiO<sub>2</sub> (Figure 1a). One can consider CNs, able to store electrons upon light irradiation, as finely designed enzyme-like architectures, which brings us to the concept of IDEASE, Illumination-Driven Electron Accumulation in Semiconductors and Exploitation. The analogy becomes more evident if we refer to photosynthesis, which can be schematically represented as a two-step process. In phase I, or the light phase, CNs accumulate electrons, in the process under the IDEAS acronym,<sup>[99g]</sup> as previously introduced by Savateev and co-workers. After that follows phase II, or Dark phase. Here the stored electrons are exploited in different ways (Figure 6a).

Depending on the use of these stored charges, different applications are found in literature and even more can be created. It should be noted that charge and discharge processes in PHI materials differ from previously reported semiconductor-metal composites, since in this case it is more appropriate to talk about solvated electrons delocalized over organic hetero-aromatic heptazine units, rather than metal nanoparticles studied earlier by Kamat et al.<sup>[110]</sup>

Therefore, the acronym IDEASE is a convenient and short term to define such a biomimetic multi step process.<sup>[99g,m,n]</sup> Lotsch, Jeschke, Reisner and co-workers found that during the dark phase, once charged with electrons during irradiation in presence of benzylic alcohol, CN materials enable HER with the aid of colloidal Pt (Figure 6b).<sup>[99n]</sup> Thanks to this work, it is now possible to brand photocatalytic net reductive reactions, in which photocatalyst turnover is accomplished in dark, with the name “Dark Photocatalysis”. It has been also shown that the long-lived radicals can be generated by applying cathodic voltage. The continuous charging can be seen as a super-capacitor, suggesting that energy transfer via carbon nitride in a sort of solar battery may be possible.

Indeed, straight after discovery of “Dark Photocatalysis”, Lotsch and co-workers built a solar half-battery based on cyanamide-functionalized PHI (NCN-PHI) (Figure 6c).<sup>[99m]</sup> When a NCN-PHI based electrode is illuminated in the presence of benzylic alcohol, the voltage in open circuit potential (OCP) measurements raises up to  $-0.6$  vs. NHE and can be discharged in dark. It is also possible to perform charge and discharge cycles only using electricity as the driving force (in permanent dark conditions). Furthermore, it must also be pointed out that PHIs are able to absorb light and store/discharge photoinduced electrons in one single carbon nitride material, with no need of further electron shuttles.

Savateev and co-workers quantified the capacity of PHI materials in IDEAS by titration of the long-lived radical with methyl viologen (MV<sup>2+</sup>) (Figure 6d).<sup>[99g]</sup> In their work, they used K-PHI and benzyl amine as an electron donor. Experimentally, it was found that 1 gram of K-PHI is able to store up to at least 0.95 mmol of electrons corresponding to one uncoupled electron per four heptazine units. Wang and co-workers exploited the discussed phenomenon in the reduction of molecular oxygen in the presence of a proton source for the

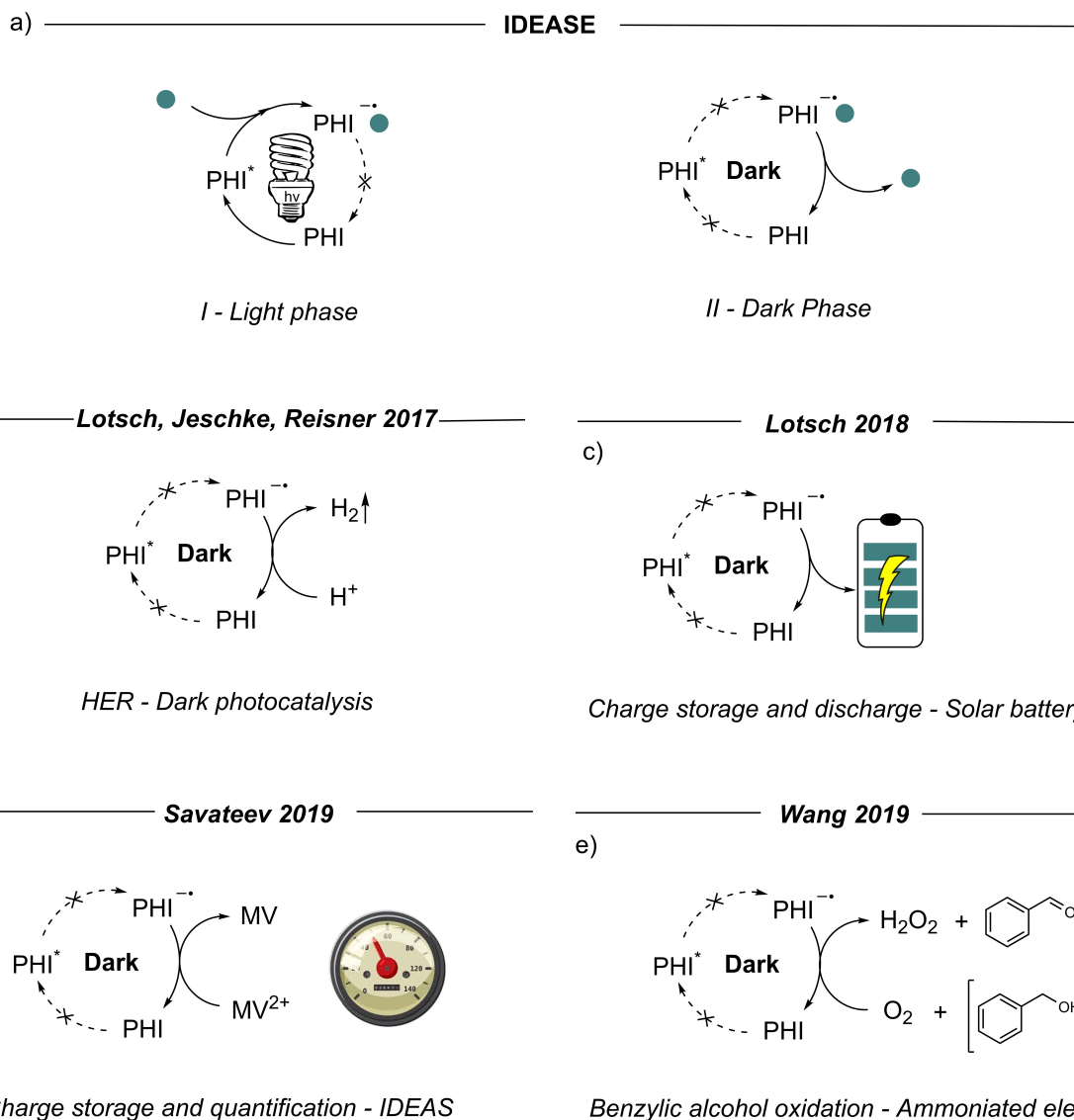


Figure 6. Various examples of the IDEASE concept.

generation of  $\text{H}_2\text{O}_2$ , using benzyl alcohol as hole scavenger, which is further oxidized to benzaldehyde (Figure 6e).<sup>[101]</sup> Therefore, it may be considered as another example of Dark Photocatalysis. Although such long-lived radicals are known since a discrete amount of time and not only related to CN materials,<sup>[111]</sup> the combination of this feature with other properties of carbon nitrides will yield a number of applications in photocatalysis and beyond.

### 3. Energy transfer in Carbon Nitrides

Energy transfer is defined as the photophysical process where an excited state of a molecular species (donor) is quenched by another molecule (acceptor), increasing its energy.<sup>[112]</sup> Related to the topic of present review, the term 'donor' refers to photocatalyst or photosensitizer.

For this process to happen, it is fundamental that the photocatalyst, once in its excited state, is able to perform an intersystem crossing (ISC) forming a triplet excited state ( $S_1-T_1$  transition). Relaxation of the photocatalyst triplet to the ground state ( $T_1-S_0$  intersystem crossing) is spin forbidden and is therefore a much slower process compared to  $S_1-S_0$  transition, which guarantee extensive excited state lifetime to participate in bimolecular quenching processes.<sup>[113]</sup> The employment of a visible light photosensitizer is convenient as they are able to access the triplet excited state under less energetic electromagnetic radiation, which is beneficial for higher selectivity and the scope of functional groups tolerated in the specific photocatalytic reaction.<sup>[114]</sup> Energy transfer processes are also differentiated in two categories: 1) Förster Resonance Energy Transfer (FRET) due to dipole-dipole interactions, a process which plays an important role in photosynthesis, fluorescence labeling and bioimaging; 2) Dexter Energy transfer, due to a simultaneous exchange of electrons between acceptor ground state and

donor excited state respectively, a process which dominates photosensitized organic reactions in solution.<sup>[9]</sup>

One peculiarity of the photocatalytic mechanism based on energy transfer, is that it does not generate charged ions, which nevertheless are implied in the mechanism based on electron transfer (Figure 7a).<sup>[97]</sup> Extensive literature analysis suggests that a vast majority of photocatalytic reactions mediated by carbon nitrides are explained in terms of pure electron transfer, while energy transfer is not even considered.<sup>[71]</sup> However, the conjugated polymer structure of carbon nitrides is similar to that of polyaromatic compounds, which might be beneficial for singlet-triplet ISC.<sup>[9]</sup> Therefore, the energy transfer mechanism for carbon nitrides can also be operative. K-PHI is characterized by a relatively short fluorescence lifetime ( $S_1$ - $S_0$  transition)  $\tau_{FL}$  = 600 ps and a fluorescence quantum efficiency (QE) < 0.1 % that supports the existence of non-radiative pathways of the excited state relaxation.<sup>[99b]</sup> At the same time, for covalent carbon nitrides typically  $\tau_{FL}$  > 2 ns and fluorescence QE > 10% have been reported.<sup>[105b,115]</sup> Since the yield of free ions is higher for triplet contact radical ion pair,<sup>[79]</sup> the ability of the sensitizer to form a long-lived triplet state, which can be achieved by decreasing singlet-triplet energy gap, is beneficial for the photocatalytic reaction. For K-PHI as well as covalent carbon

nitrides, such singlet-triplet energy gap has been determined to be  $\sim 0.2$  eV.<sup>[114]</sup> Overall, materials with long  $\tau_{FL}$  and  $\tau_{PHr}$  short  $\tau_{ISC}$  are beneficial for application in photocatalysis.

Taking K-PHI as an example and using TA spectroscopy, in collaboration with Strauss and Guldi, we confirmed singlet-triplet ISC and described excited state dynamics with the corresponding lifetimes (Figure 7c).<sup>[99b]</sup> Compared to ionic carbon nitride such as K-PHI, in which ISC occurs within  $\tau_{ISC}$  = 470 ps and a phosphorescence lifetime of  $\tau_{PH}$  = 2.07  $\mu$ s, in covalent carbon nitride, prepared via calcining melamine, ISC has been reported to occur within few ps, while the phosphorescence lifetime is  $\sim 124$   $\mu$ s.<sup>[105b]</sup> Although, both ionic and covalent carbon nitrides belong to the same class of materials, this example illustrates that exciton dynamics in carbon nitrides could be tuned in a broad range. Huang and co-workers found that CNs can act as photosensitizers when excited with photons at 340 nm.<sup>[116]</sup> This leads to a fluorescence resonance energy transfer (FRET) to riboflavin (RF), with green emission at 532 nm (Figure 7d). After such discovery, the authors applied this concept for the development of an analytical method for the determination of RF in complex matrix samples, based on fluorescence ratiometric detection. By this method, they were able to quantify RF amount in milk and commercial vitamin

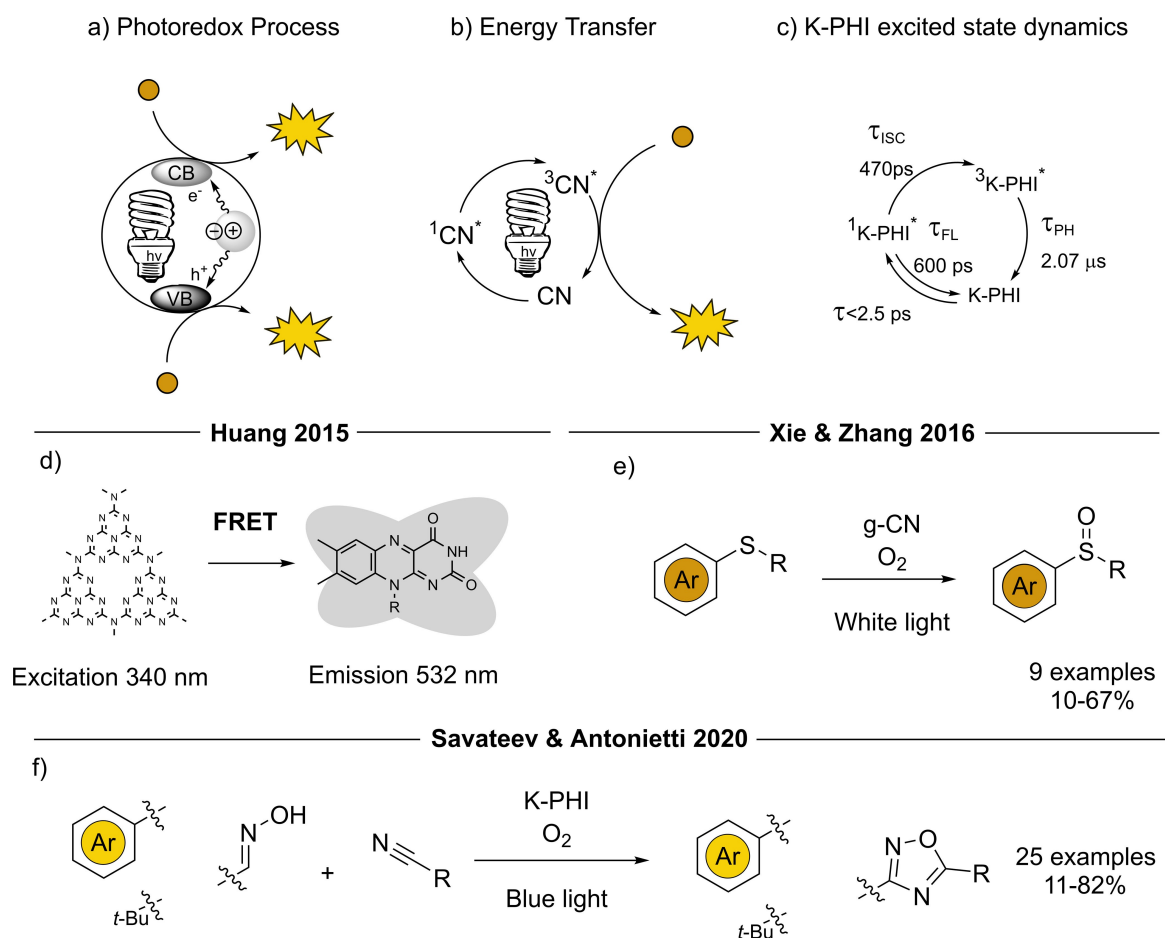


**Figure 7.** Schematic mechanisms overview and energy transfer processes reported in literature. a) Photoredox catalytic process in semiconductors. b) Energy transfer process; c) K-PHI excited state dynamics; d) FRET between g-CN and riboflavin. e) Generation of  $^1O_2$  for the synthesis of sulfoxides; f) generation of  $^1O_2$  for the preparation of oxadiazoles and isoxazoles.

drinks in a simple, economical and sensitive manner. This represent a brilliant example of using CNs as photochemical sensors. After, Xie, Zhang and co-workers proved that oxygen can serve as energy acceptor in combination with CN materials.<sup>[117]</sup> They showed that in situ generated singlet oxygen ( $^1\text{O}_2$ ) can be used to oxidize sulfides to sulfoxides (Figure 7e). Savateev and Antonietti used K-PHI in synthesis of highly valuable active pharmaceutical ingredients (APIs), such as oxadiazoles-1,2,4 and isoxazoles, via a cascade of energy transfer, which involves sensitization of  $^1\text{O}_2$  and [3+2]-cyclo-addition reaction (Figure 7f).<sup>[99b]</sup> Although only few papers report using CNs in energy transfer processes, the authors foresee the application of this feature to expand a portfolio of organic reactions mediated by  $^1\text{O}_2$  or combining CNs with other energy acceptors.

#### 4. Flow Chemistry

Flow chemistry is a chemical technology involving the employment of channels or tubing to conduct a reaction in a continuous stream, and is quickly becoming an indispensable tool and widespread technology among laboratories.<sup>[118]</sup> It guarantees unique control of key reaction parameters, ensuring efficient mixing and heat transfer, unmatched by batch technology from this point of view.<sup>[119]</sup> It is also an opportunity to scale-up reactions easily, increasing productivity by lowering the reaction times.<sup>[120]</sup> Flow technology can also be coupled with other techniques, such as organic synthesis under microwave irradiation, as has been studied in depth by Barham et al.<sup>[121]</sup>

Despite the enormous amount of literature published in the field of photocatalysis and photoredox catalysis, industrial applications, except few examples, are scarce.<sup>[122]</sup> The reason behind this is attributed mainly to a Beer-Lambert law limitation,<sup>[123]</sup> whereby increasing the size of the vessel decreases the light penetration, and thus, the net photocatalytic activity.<sup>[124]</sup> In addition, considering that photocatalysts usually employed in organic synthesis include expensive metals, synthesis of APIs by this approach become expensive.<sup>[125]</sup> In this context, CNs can be up to three orders of magnitude less expensive than other photocatalysts, and more importantly, can be recycled.<sup>[69]</sup> Efforts have been undertaken to establish CN photocatalysis in large-scale.<sup>[72c]</sup> The coupling of carbon nitride photocatalysis with a flow approach is envisioned as a promising solution to replace expensive metal photocatalysts. Colloid dispersions, such as suspension of semiconductor in liquid phase, vastly decrease light penetration due to scattering, observed in UV-vis absorption spectra as significant absorption in the full optical range.<sup>[99a]</sup> Scattering also results in a higher absorption coefficient in the Beer-Lambert equation.<sup>[126]</sup> Therefore, in heterogeneous photocatalysis, to ensure efficient light delivery into the bulk of the reaction mixture, thin flow photoreactors are a preferential choice in scale-up strategies. Three main technologies have been adopted so far in CN photocatalysis in flow (Figure 8). I) Packed bed reactors, in which the catalyst is immobilized or grafted inside the tube and reagents are pumped through the reactor. It can be considered as a simple and steady solution preventing the catalyst separation step, although these type of reactors are known to have great pressure drops, which requires high inlet pressure. In addition, clogging often occurs upon prolonged usage.<sup>[127]</sup> They also have great limitations due to light penetration – light

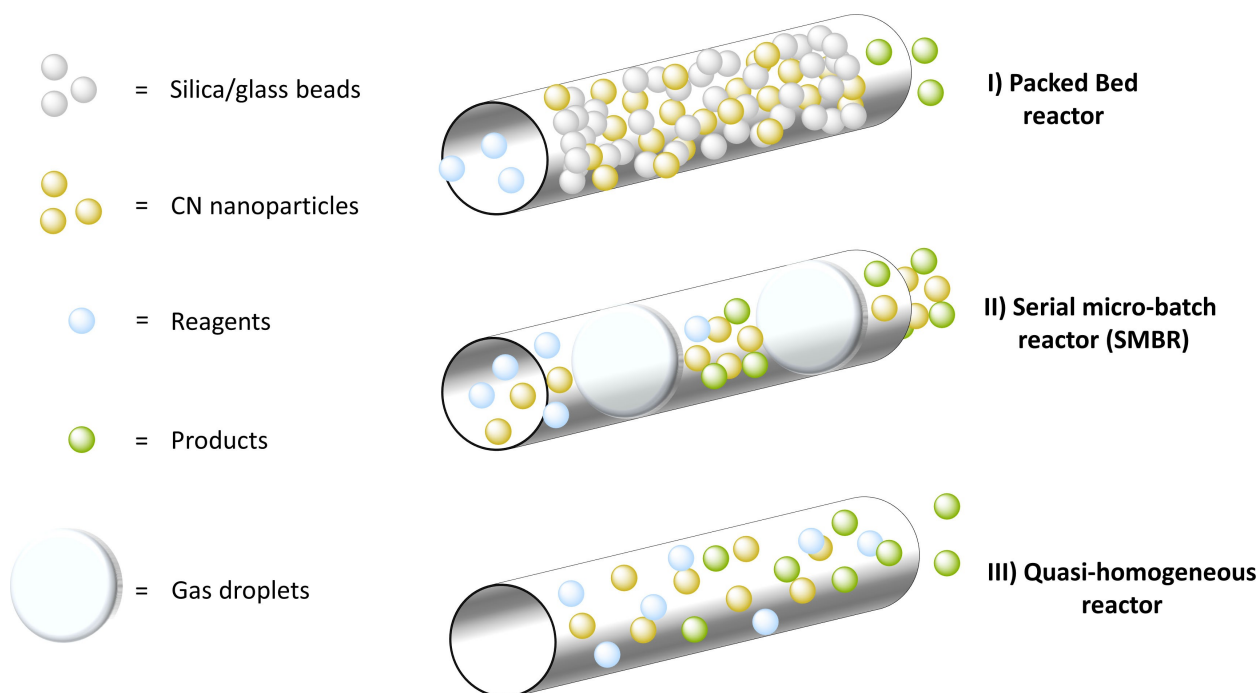
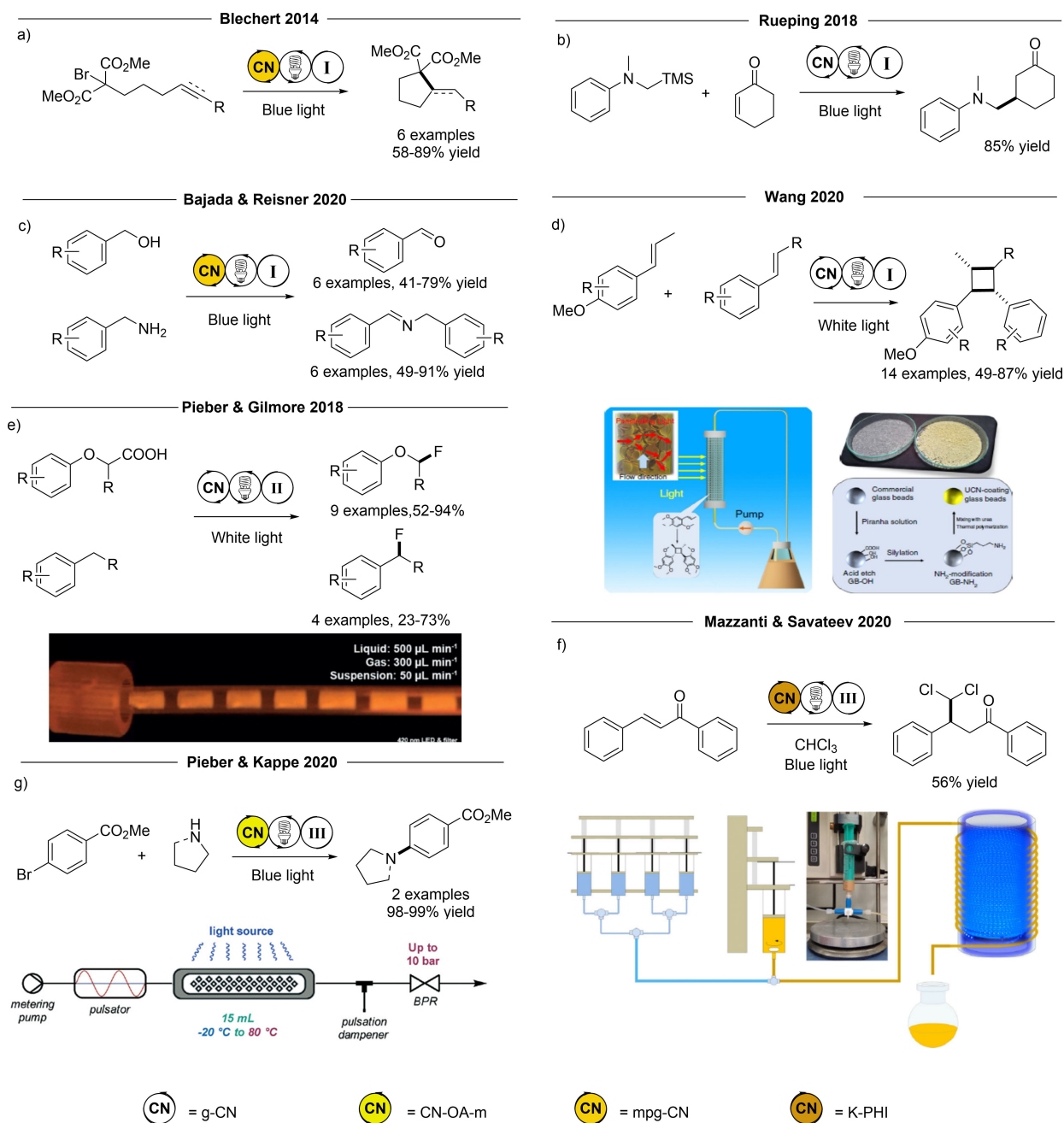


Figure 8. Overview of different technologies in carbon nitride flow photocatalysis.

reaches only the outside layers of the catalyst, which are closer to the reactor walls. II) Serial micro-batch reactor (SMBR), in which segmented gas-slurry stream is passed through the tubular reactor, is a convenient solution to mitigate the no-slip condition. However, such systems have a long onset time. In addition, since productivity correlates with the flow rate, increasing the reaction time might lead to CN deposition. III) Quasi-homogeneous photocatalysis, in which stable colloid solution composed of carbon nitride and reagents in polar solvent is pumped through the tubing, identical to the reactor

configuration in homogeneous photocatalysis. The approach is similar to SMBR, without the employment of a gas line. The strategy is still convenient for scaling up reactions, avoiding clogging, and having good irradiation surface. In the first approach, Blechert and co-workers used a packed bed reactor filled with mpg-CN, silica and glass beads (to reduce back pressure).<sup>[95c]</sup> This technology was tested in radical cyclisation of 2-bromo-1,3-dicarbonyl compounds (Figure 9a). Using the flow reactor, reaction time was shortened by about fifty times, 5 min versus 4 h, compared to the reaction in batch.



**Figure 9.** CN photo-flow chemistry. Different scale-up methodologies for photochemical reactions and improve productivities. Inset in d) is reproduced and modified from reference [128] with permission from Springer Nature. Inset in e) is reproduced and modified from reference [140] with permission from Wiley-VCH. Inset in f) is reproduced and modified from reference [99a] with permission from Springer Nature. Inset in g) is reproduced and modified from [131] with permission from The Royal Society of Chemistry.

Years later Rueping et al. reported an analogous technology, by using a chromatography column, with a similar filler composition, but employing g-CN as the photocatalyst (Figure 9b).<sup>[94b]</sup> Accordingly, the flow approach reduced reaction time by about six times, 3 h versus 17 h, in the photocatalyzed desilylative addition of  $\alpha$ -silylamines.

Reisner and co-workers built a packed bed photoreactor similar to the aforementioned one, but employed it in a triphasic gas-liquid-solid flow system with oxygen as the gaseous phase.<sup>[95a]</sup> Overall, this technology demonstrated 3–6 times higher productivity, with higher conversion of benzylamines in homocoupling and benzylic alcohols oxidation (12 examples), but lower selectivity compared to the reaction in batch (Figure 9c).

Wang, Zhang and co-workers grafted CN material as a film on silica beads, in order to increase catalyst surface area and the area exposed to light.<sup>[128]</sup> This approach increased productivity by 10 times compared to the reaction in batch in the [2 + 2] dimerization of  $\alpha$ -sarone in gram scale (Figure 9d).

Pieber and Gilmore developed SMBR concept in decarboxylative fluorination of carboxylic acids.<sup>[129]</sup> In decarboxylative fluorination of phenoxyacetic acid to (fluoromethoxy)benzene, as an example, the productivity was increased 5 times compared to the approach in batch (Figure 9e). The approach allows for efficient mixing inside the individual slurry segment,<sup>[127]</sup> while segmented flow eliminates the problem of no-slip condition, reactor clogging, catalyst leaching, and deposition. In addition, due to higher interface area between gaseous and liquid phase, the approach holds promise for photocatalytic reactions employing O<sub>2</sub>.

Krivtsov, Beranev, and co-workers introduced 'quasi-homogeneous photocatalysis' concept, according to which heptazine-based polymeric carbon nitrides nanoparticles with size  $10 \pm 3$  nm are used as water-soluble photocatalyst, but at the same time can be recovered by simple modulation of the ionic strength of the medium.<sup>[130]</sup>

Mazzanti, Savateev and coworkers, employed exceptional properties of K-PHI to form stable colloid solution in polar solvents, namely highly negative zeta-potential of  $-40$  mV, in the flow photoreactor with the design similar to that used in homogeneous photocatalysis (Figure 9f).<sup>[99a]</sup> At the same time, the average diameter of K-PHI particles is 100 nm, enabling simple recovery of the photocatalyst from the reaction mixture via centrifugation. Using this concept, authors increased productivity of  $\gamma,\gamma$ -dichloroketones synthesis from  $\alpha,\beta$ -unsaturated ketones, chloroform and triethanolamine by 19 times compared to the reaction in batch.

Looking at the problem of catalyst dispersion from another point of view, instead of the exploitation of material colloidal properties, Kappe, Pieber, and co-workers employed an oscillatory plug flow photoreactor in heterocoupling of alkyl amines with aryl bromides (Figure 9g).<sup>[131]</sup> Authors reached grams-per-hour productivity, which is 24 times higher compared to the reaction in batch. This particular approach is free of moving parts, allows for the pumping of dispersion containing reagents and CN catalyst directly through the reactor, and prevents settling of solid material.

Although described herein, flow technologies are based on either a specific property of CN photocatalysts, such as high stability of colloid solution, or dedicated hardware, all of them univocally support higher productivity (gram of product per hour) of flow approach compared to the reaction in batch.<sup>[118,132]</sup> CN flow chemistry ensures much higher photon efficiency compared to batch reactions. Future development of this field combined with CNs will be soon extended in combination with the expanding topics of gas-liquid phase photoredox catalysis and PEC.<sup>[6a,120c]</sup>

## 5. Photoredox Metal/Dual Catalysis

Complexes of palladium remain the most commonly used catalysts in different types of cross-coupling reactions.<sup>[133]</sup> However, due to the high price of palladium, resources of the catalysis community are concentrated on development of catalytic protocols based on more abundant elements, such as Ni.<sup>[134]</sup> The intrinsic problem of using Ni in catalysis is the inability of Ni(II)-species to undergo efficiently reductive elimination to complete the catalytic cycle, and high stability of Ni(I)-species formed upon reductive elimination of the cross-coupling product unless complex ligands and strong bases are employed.<sup>[135]</sup> An alternative approach is envisioned in merging Ni-catalysis with photoredox active complex, as has been proposed by Molander et al., in which photoredox active complex reduces Ni(II) to Ni(0) and therefore closes the catalytic cycle.<sup>[136,137]</sup> Pd can be replaced by Ni in dual photoredox catalysis, where typically expensive Ir-complexes are used as the photoredox active partner.<sup>[138]</sup>

In this view carbon nitrides, although they are intrinsically free of transition metals, also hold tremendous promise as a photoredox component in dual nickel/carbon nitride catalysis. It should be noted that while design of carbon nitride materials doped with single metal atoms or metal clusters has been a central topic of research, still such materials are mainly used in environmental applications and water splitting, which is beyond the scope of this review.<sup>[91,97]</sup>

Related to dual Ni-carbon nitride photocatalysis in organic synthesis, Reisner, Durrant, Lotsch and co-workers, reported oxidation of benzylic alcohols coupled with HER using <sup>N</sup>CN<sub>x</sub> and nickel molecular complex as co-catalysts (Figure 10a).<sup>[98]</sup>

Later, Vijeta and Reisner reported Minisci reaction coupled with HER, using <sup>N</sup>CN<sub>x</sub> and Pt nanoparticles (Figure 10b).<sup>[139]</sup> Pieber and co-workers combined CN-OA-m (a type of CN material prepared by condensation of urea and oxamide) with an in-situ formed Ni complex to achieve esterification of carboxylic acids with aryl iodides.<sup>[140]</sup> Immediately after, the same group extended the method to synthesize thioethers and ethers via coupling of alcohols and thiols with aryl bromides and iodides (Figure 10c).<sup>[141]</sup> Ghosh, König, Antonietti and co-workers combined mpg-CN with Ni in C–N coupling of aryl halides with aliphatic/aromatic amines and sulfamides (Figure 10d), without the employment of any additional ligand.<sup>[95f]</sup> Apart from C-heteroatom coupling, Khamrai, König, Antonietti and co-workers reported C–C coupling between aryl halides

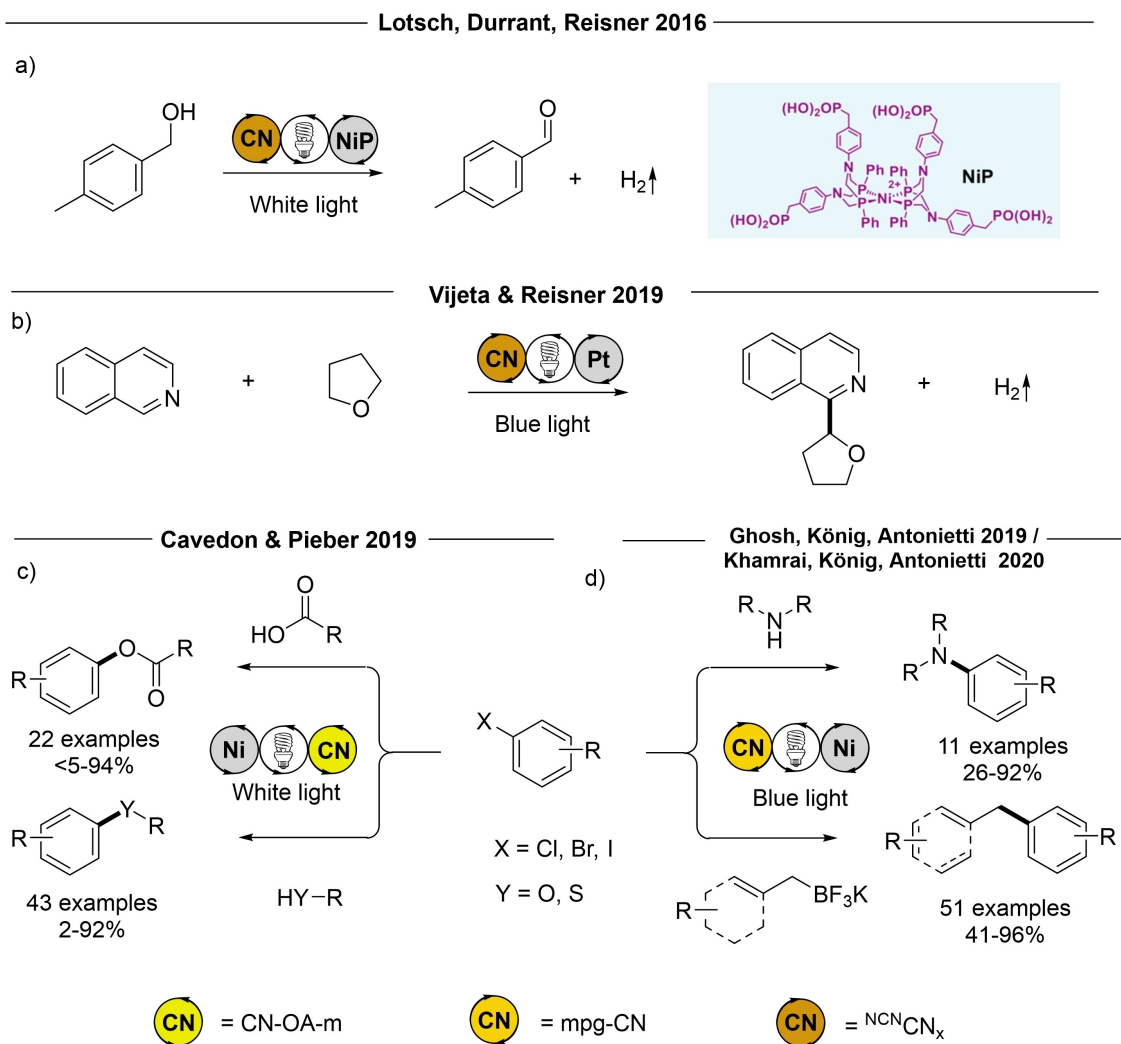


**Figure 10.** Overview of photoredox metal/dual catalysis. a) Benzylic alcohol oxidation reported from Reisner and co-workers. Inset in a) reproduced and modified from reference [98] with permission from American Chemical Society. b) Minisci reaction from Reisner and co-workers. c) C–O and C–S cross coupling from Pieber and co-workers. d) C–N cross coupling from König and Antonietti and C–C coupling from König and co-workers.

and potassium alkyl trifluoroborates (Figure 10d) using mpg-CN and Ni.<sup>[95b]</sup> Although the mechanism has not been investigated in details, by making a comparison with the homogeneous version of dual Ni/photoredox catalysis, authors postulate that in the first step, excitation of mpg-CN yields ‘two-dimensional surface redox centers as electron-hole pairs’. The hole oxidizes trifluoroborate and gives benzylic radical, which in turn is trapped by Ni<sup>II</sup> complex generated upon aryl halide oxidative addition to Ni<sup>0</sup> catalyst. Reductive elimination of the coupling product delivers Ni<sup>I</sup> complex that is reduced by the photo-generated electron to Ni<sup>0</sup> catalyst. Alternatively, Ni<sup>0</sup> can trap benzylic radicals to generate more stable Ni<sup>I</sup> complex and perform subsequent oxidative addition of an aryl halide, providing Ni<sup>III</sup> complex.<sup>[136]</sup>

Nocera and co-workers reported carbon nitride in C–N (without addition of ligand) and C–O (with addition of ligand) couplings.<sup>[142]</sup>

Using broad absorption of CN-OA-m,<sup>[102]</sup> Gisbertz and Pieber developed a protocol for C–N coupling of electron rich

arylbromides with amines under green light that overcomes a problem of nickel-black formation and subsequent deactivation of the photocatalyst.<sup>[143]</sup>

Although until now carbon nitrides have been successfully coupled mostly with Ni and once with Pt in organic photoredox catalysis, the approach can potentially be extended on other earth-abundant metals to address existing challenges in functionalization of organic molecules.

## 6. Summary and Outlook

Carbon nitride photocatalysis is full of intriguing concepts applicable to the needs of photocatalysis. IDEASE allows for temporary electron storage in ionic carbon nitrides triggered by irradiation with visible light. The electrons are then used in different redox reactions.

Although electron transfer is commonly used to explain photocatalytic mechanism, recent results indicate that the CN

excited state also undergoes singlet-triplet intersystem crossing followed by energy transfer to a suitable molecule. However, reports are limited mainly to O<sub>2</sub> that in this process is converted to <sup>1</sup>O<sub>2</sub>. Excited state dynamics is governed by the CN material structure, and can be broadly tuned. Based on the available, but not numerous reports, we conclude that in general more amorphous CNs demonstrate longer phosphorescence lifetime and faster ISC.

Plentiful examples in C–N, C–C and C–O coupling mediated by Ni/carbon nitride dual photocatalysis clearly demonstrate that this photocatalytic system can efficiently replace rare metal photoredox complexes, which makes the concept especially appealing for application in organic photoredox catalysis on large-scale.

In this view, enabling the chemical process in flow complements carbon nitride photocatalysis in scaling up the reaction. Several architectures of flow reactors have been proposed, to account for heterogeneous nature of carbon nitride photocatalysis. These are classical packed bed flow photoreactors as well as more innovative concepts – serial microbatch reactors, and oscillatory plug flow photoreactor. At the same time, processing of carbon nitride materials gives rise to the concept of flow photocatalysis in quasi-homogeneous fashion.

Taking into consideration progress in fabrication of thin carbon nitride films by chemical vapor deposition, we envision this approach to be also extremely useful for the fabrication of flow photoreactors coated with light-responsive material from the family of carbon nitrides.

Although design of carbon nitride materials remains one of the hottest topics in materials chemistry, focus gradually shifts toward application of these materials in synthesis of APIs and development of synthetic protocols for synthesis of value-added organic compounds. At the same time, advanced time resolved spectroscopic techniques, such as TAS and TRPL, are becoming indispensable tools for understanding the underpinning mechanism of photocatalytic transformations and is the foundation for rational design of photocatalysts.<sup>[144]</sup> Based on our many-year experience of working in the field of carbon nitride photocatalysis, we believe this trend will increase in future.

At the same time, a multitude of research in water splitting via PEC on one hand and organic photoredox catalysis in suspended systems on the other hand, might lead to merging of these approaches into photoelectrochemical organic synthesis employing CN based photoelectrodes.

## Acknowledgements

We gratefully acknowledge the Max Planck Society for financial support. The Deutsche Forschungsgemeinschaft is gratefully acknowledged for providing financial support for this project (DFG-An 156 13-1). The authors thank Prof. Markus Antonietti for fruitful discussion during preparation of the review. Prof. Xinchen Wang and Dr. Lihua Lin are acknowledged for providing SEM, TEM, PXRD and crystal structure images of PTI/Li<sup>+</sup>Cl<sup>-</sup>. The authors are deeply thankful to Bradley D. Frank for his efforts in improving

the language in order to reach a broad readership. Open access funding enabled and organized by Projekt DEAL.

## Conflict of Interest

A patent WO/2019/081036 has been filed by Max Planck Gesellschaft zur Förderung der Wissenschaften E.V. in which AS is listed as a co-author.

**Keywords:** carbon nitrides · energy transfer · flow chemistry · photocatalysis · radical chemistry

- [1] K. Kubota, Y. Pang, A. Miura, H. Ito, *Science* **2019**, 366, 1500.
- [2] a) M. Ghosh, V. S. Shinde, M. Rueping, *Beilstein J. Org. Chem.* **2019**, 15, 2710–2746; b) E. J. Horn, B. R. Rosen, P. S. Baran, *ACS Cent. Sci.* **2016**, 2, 302–308; c) M. D. Kärkäs, *Chem. Soc. Rev.* **2018**, 47, 5786–5865.
- [3] A. Nicewicz, D. W. C. MacMillan, *Science* **2008**, 322, 77–80.
- [4] a) D. S. Achilleos, W. Yang, H. Kasap, A. Savateev, Y. Markushyna, J. R. Durrant, E. Reisner, *Angew. Chem. Int. Ed. Engl.* **2020**, 59, 18184–18188, *Angew. Chem.* **2020**, 132, 18341–18345; b) T. Uekert, H. Kasap, E. Reisner, *J. Am. Chem. Soc.* **2019**, 141, 15201–15210.
- [5] a) T. Koike, M. Akita, *Synlett* **2013**, 24, 2492–2505; b) S. Crespi, M. Fagnoni, *Chem. Rev.* **2020**, 120, 9790–9833.
- [6] a) J. P. Barham, B. König, *Angew. Chem. Int. Ed. Engl.* **2020**, 59, 11732–11747, *Angew. Chem.* **2020**, 132, 11828–11844; b) L. Marzo, S. K. Pagire, O. Reiser, B. König, *Angew. Chem. Int. Ed. Engl.* **2018**, 57, 10034–10072, *Angew. Chem.* **2018**, 130, 10188–10228.
- [7] R. H. Verschuere, W. M. De Borggraeve, *Molecules* **2019**, 24.
- [8] A. García, C. Fernandez-Blanco, J. R. Herance, J. Albero, H. García, *J. Mater. Chem. A* **2017**, 5, 16522–16536.
- [9] F. Strieth-Kalthoff, M. J. James, M. Teders, L. Pitzer, F. Glorius, *Chem. Soc. Rev.* **2018**, 47, 7190–7202.
- [10] F. Glaser, C. Kerzig, O. S. Wenger, *Angew. Chem. Int. Ed. Engl.* **2020**, 59, 10266–10284, *Angew. Chem.* **2020**, 132, 10350–10370.
- [11] A. Pannwitz, O. S. Wenger, *Chem. Commun. (Camb.)* **2019**, 55, 4004–4014.
- [12] a) T. S. Teets, *Iridium(III) in Optoelectronic and Photonics Applications*, (Ed: E. Zysman-Colman), John Wiley & Sons, **2018**; b) D. M. Hedstrand, W. H. Kruizinga, R. M. Kellogg, *Tetrahedron Lett.* **1978**, 19, 1255–1258; c) H. Cano-Yelo, A. Deronzier, *Tetrahedron Lett.* **1984**, 25, 5517–5520.
- [13] a) O. S. Wenger, *J. Am. Chem. Soc.* **2018**, 140, 13522–13533; b) C. Förster, K. Heinze, *Chem. Soc. Rev.* **2020**, 49, 1057–1070; c) A. Hossain, A. Bhattacharyya, O. Reiser, *Science* **2019**, 364, DOI 10.1126/science.aav9713.
- [14] a) V. Mojir, E. Svobodová, K. Straková, T. Neveselý, J. Chudoba, H. Dvořáková, R. Cibulka, *Chem. Commun. (Camb.)* **2015**, 51, 12036–12039; b) J. Zelenka, E. Svobodová, J. Tarábek, I. Hoskovicová, V. Boguschová, S. Bailly, M. Sikorski, J. Roithová, R. Cibulka, *Org. Lett.* **2019**, 21, 114–119; c) I. K. Sideri, E. Voutrytsa, C. G. Kokotos, *Org. Biomol. Chem.* **2018**, 16, 4596–4614.
- [15] D. A. Nicewicz, T. M. Nguyen, *ACS Catal.* **2014**, 4, 355–360.
- [16] a) K. A. Korvinson, G. N. Hargenrader, J. Stevanovic, Y. Xie, J. Joseph, V. Maslak, C. M. Hadad, K. D. Glusac, *J. Phys. Chem. A* **2016**, 120, 7294–7300; b) Friedmann, A. Hakki, H. Kim, W. Choi, D. Bahnemann, *Green Chem.* **2016**, 18, 5391–5411; c) S. Kohtani, A. Kawashima, H. Miyabe, *Front. Chem.* **2019**, 7:630, DOI 10.3389/fchem.2019.00630; d) D. W. Manley, J. C. Walton, *Beilstein J. Org. Chem.* **2015**, 11, 1570–1582.
- [17] S. Sohrabi, M. K. Moraveji, D. Iranshahi, *Rev. Chem. Eng.* **2019**, 36, 687–722.
- [18] a) K. Fuku, N. Wang, Y. Miseki, T. Funaki, K. Sayama, *ChemSusChem* **2015**, 8, 1593–1600; b) H. Tateno, Y. Miseki, K. Sayama, *ChemElectroChem* **2017**, 4, 3283–3287.
- [19] G. Beck, M. Sieland, J. F. Beleites, R. Marschall, B. M. Smarsly, *Inorg. Chem.* **2019**, 58, 2599–2609.
- [20] A. L. Luna, F. Matter, M. Schreck, J. Wohlwend, E. Tervoort, C. Colbeau-Justin, M. Niederberger, *Appl. Catal. B* **2020**, 267, 118660.



- [21] a) M. Monai, T. Montini, P. Fornasiero, *Catalysts* **2017**, *7*, 304; b) T. Montini, M. Melchionna, M. Monai, P. Fornasiero, *Chem. Rev.* **2016**, *116*, 5987–6041.
- [22] Y. Lin, J. Guo, J. San Martin, C. Han, R. Martinez, Y. Yan, *Chem. Eur. J.* **2020**, *26*, 13118–13136.
- [23] a) A. Dhakshinamoorthy, A. M. Asiri, H. Garcia, *Adv. Mater.* **2019**, *31*, 1900617; b) D. Mateo, A. Santiago-Portillo, J. Albero, S. Navalón, M. Alvaro, H. García, *Angew. Chem. Int. Ed. Engl.* **2019**, *58*, 17843–17848, *Angew. Chem.* **2019**, *131*, 18007–18012.
- [24] A. Dhakshinamoorthy, A. M. Asiri, H. Garcia, *ACS Catal.* **2017**, *7*, 2896–2919.
- [25] X. Deng, Z. Li, H. Garcia, *Chem. Eur. J.* **2017**, *23*, 11189–11209.
- [26] S. Abednatanzi, P. Gohari Derakhshandeh, H. Depauw, F.-X. Coudert, H. Vrielinck, P. Van Der Voort, K. Leus, *Chem. Soc. Rev.* **2019**, *48*, 2535–2565.
- [27] B. Ohtani, *Catalysts* **2013**, *3*, 942–953.
- [28] a) D. Noureldine, K. Takanabe, *Catal. Sci. Technol.* **2016**, *6*, 7656–7670; b) K. Watanabe, A. Iwase, A. Kudo, *Chem. Sci.* **2020**, *11*, 2330–2334.
- [29] M. Weiss, B. Wirth, R. Marschall, *Inorg. Chem.* **2020**, *59*, 8387–8395.
- [30] a) K. Kirchberg, R. Marschall, *Sustainable Energy & Fuels* **2019**, *3*, 1150–1153; b) R. A. Henning, P. Uredat, C. Simon, A. Bloesser, P. Cop, M. T. Elm, R. Marschall, *J. Phys. Chem. C* **2019**, *123*, 18240–18247.
- [31] a) K. Obata, Y. Shinohara, S. Tanabe, I. Waki, K. Kotsosovos, K. Ohkawa, K. Takanabe, *Energy Technol.* **2019**, *7*, 1900575; b) Y. Goto, T. Hisatomi, Q. Wang, T. Higashi, K. Ishikiriyama, T. Maeda, Y. Sakata, S. Okunaka, H. Tokudome, M. Katayama, S. Akiyama, H. Nishiyama, Y. Inoue, T. Takewaki, T. Setoyama, T. Minegishi, T. Takata, T. Yamada, K. Domen, *Joule* **2018**, *2*, 509–520.
- [32] a) Z. Wang, C. Li, K. Domen, *Chem. Soc. Rev.* **2019**, *48*, 2109–2125; b) K. Takanabe, *ACS Catal.* **2017**, *7*, 8006–8022; c) Q. Wang, K. Domen, *Chem. Rev.* **2020**, *120*, 919–985.
- [33] J. Byun, K. A. I. Zhang, *Mater. Horiz.* **2020**, *7*, 15–31.
- [34] C. Krishnaraj, H. S. Jena, K. Leus, P. Van Der Voort, *Green Chem.* **2020**, *22*, 1038–1071.
- [35] W. Huang, J. Byun, I. Rörich, C. Ramanan, P. W. M. Blom, H. Lu, D. Wang, L. Caire da Silva, R. Li, L. Wang, K. Landfester, K. A. I. Zhang, *Angew. Chem. Int. Ed. Engl.* **2018**, *57*, 8316–8320, *Angew. Chem.* **2018**, *130*, 8449–8453.
- [36] Z. J. Wang, S. Ghasimi, K. Landfester, K. A. I. Zhang, *J. Mater. Chem. A* **2014**, *2*, 18720–18724.
- [37] L. Wang, W. Huang, R. Li, D. Gehrig, P. W. M. Blom, K. Landfester, K. A. I. Zhang, *Angew. Chem. Int. Ed. Engl.* **2016**, *55*, 9783–9787, *Angew. Chem.* **2016**, *128*, 9935–9940.
- [38] R. Li, B. C. Ma, W. Huang, L. Wang, D. Wang, H. Lu, K. Landfester, K. A. I. Zhang, *ACS Catal.* **2017**, *7*, 3097–3101.
- [39] R. Li, Z. J. Wang, L. Wang, B. C. Ma, S. Ghasimi, H. Lu, K. Landfester, K. A. I. Zhang, *ACS Catal.* **2016**, *6*, 1113–1121.
- [40] Z. J. Wang, S. Ghasimi, K. Landfester, K. A. I. Zhang, *Adv. Synth. Catal.* **2016**, *358*, 2576–2582.
- [41] a) H. Wang, H. Wang, Z. Wang, L. Tang, G. Zeng, P. Xu, M. Chen, T. Xiong, C. Zhou, X. Li, D. Huang, Y. Zhu, Z. Wang, J. Tang, *Chem. Soc. Rev.* **2020**, *49*, 4135–4165; b) R. Dawson, A. I. Cooper, D. J. Adams, *Prog. Polym. Sci.* **2012**, *37*, 530–563; c) G.-B. Wang, S. Li, C.-X. Yan, F.-C. Zhu, Q.-Q. Lin, K.-H. Xie, Y. Geng, Y.-B. Dong, *J. Mater. Chem. A* **2020**, *8*, 6957–6983.
- [42] X. Wang, S. Blechert, M. Antonietti, *ACS Catal.* **2012**, *2*, 1596–1606.
- [43] M. Shalom, S. Inal, C. Fettkenhauer, D. Neher, M. Antonietti, *J. Am. Chem. Soc.* **2013**, *135*, 7118–7121.
- [44] T. Jordan, N. Fechner, J. Xu, T. J. K. Brenner, M. Antonietti, M. Shalom, *ChemCatChem* **2015**, *7*, 2826–2830.
- [45] L. Li, Y. Zhao, M. Antonietti, M. Shalom, *Small* **2016**, *12*, 6090–6097.
- [46] J. Xu, T. J. K. Brenner, L. Chabanne, D. Neher, M. Antonietti, M. Shalom, *J. Am. Chem. Soc.* **2014**, *136*, 13486–13489.
- [47] J. Xu, H. Wang, C. Zhang, X. Yang, S. Cao, J. Yu, M. Shalom, *Angew. Chem. Int. Ed. Engl.* **2017**, *56*, 8426–8430, *Angew. Chem.* **2017**, *129*, 8546–8550.
- [48] L. Li, M. Shalom, Y. Zhao, J. Barrio, M. Antonietti, *J. Mater. Chem. A* **2017**, *5*, 18502–18508.
- [49] J. Barrio, M. Shalom, *ChemCatChem* **2018**, *10*, 5573–5586.
- [50] a) F. Dong, Z. Wang, Y. Sun, W.-K. Ho, H. Zhang, *J. Colloid Interface Sci.* **2013**, *401*, 70–79; b) S. C. Yan, Z. S. Li, Z. G. Zou, *Langmuir* **2009**, *25*, 10397–10401; c) K. Maeda, X. Wang, Y. Nishihara, D. Lu, M. Antonietti, K. Domen, *J. Phys. Chem. C* **2009**, *113*, 4940–4947; d) G. Zhang, J. Zhang, M. Zhang, X. Wang, *J. Mater. Chem.* **2012**, *22*, 8083–8091; e) H. Ji, F. Chang, X. Hu, W. Qin, J. Shen, *Chem. Eng. J.* **2013**, *218*, 183–190.
- [51] a) H. Yan, *Chem. Commun. (Camb.)* **2012**, *48*, 3430–3432; b) X. Wang, K. Maeda, X. Chen, K. Takanabe, K. Domen, Y. Hou, X. Fu, M. Antonietti, *J. Am. Chem. Soc.* **2009**, *131*, 1680–1681; c) X. Chen, Y.-S. Jun, K. Takanabe, K. Maeda, K. Domen, X. Fu, M. Antonietti, X. Wang, *Chem. Mater.* **2009**, *21*, 4093–4095.
- [52] a) H. Yan, Y. Chen, S. Xu, *Int. J. Hydrogen Energy* **2012**, *37*, 125–133; b) Y. Guo, S. Chu, S. Yan, Y. Wang, Z. Zou, *Chem. Commun.* **2010**, *46*, 7325–7327; c) B. Kumru, M. Antonietti, B. V. K. J. Schmidt, *Langmuir* **2017**, *33*, 9897–9906.
- [53] a) Z. Ding, X. Chen, M. Antonietti, X. Wang, *ChemSusChem* **2011**, *4*, 274–281; b) X. Wang, X. Chen, A. Thomas, X. Fu, M. Antonietti, *Adv. Mater.* **2009**, *21*, 1609–1612; c) G. Zhang, M. Zhang, X. Ye, X. Qiu, S. Lin, X. Wang, *Adv. Mater.* **2014**, *26*, 805–809; d) J. Zhang, J. Sun, K. Maeda, K. Domen, P. Liu, M. Antonietti, X. Fu, X. Wang, *Energy Environ. Sci.* **2011**, *4*, 675–678; e) Y. Zhang, M. Antonietti, *Chem. Asian J.* **2010**, *5*, 1307–1311; f) S. C. Yan, Z. S. Li, Z. G. Zou, *Langmuir* **2010**, *26*, 3894–3901; g) Y. Wang, Y. Di, M. Antonietti, H. Li, X. Chen, X. Wang, *Chem. Mater.* **2010**, *22*, 5119–5121; h) G. Liu, P. Niu, C. Sun, S. C. Smith, Z. Chen, G. Q. Lu, H.-M. Cheng, *J. Am. Chem. Soc.* **2010**, *132*, 11642–11648; i) J. Zhang, M. Zhang, S. Lin, X. Fu, X. Wang, *J. Catal.* **2014**, *310*, 24–30; j) G. Zhang, X. Wang, *J. Catal.* **2013**, *307*, 246–253; k) J. Zhang, G. Zhang, X. Chen, S. Lin, L. Möhlmann, G. Dołęga, G. Lipner, M. Antonietti, S. Blechert, X. Wang, *Angew. Chem. Int. Ed. Engl.* **2012**, *51*, 3183–3187, *Angew. Chem.* **2012**, *124*, 3237–3241; l) J. Zhang, X. Chen, K. Takanabe, K. Maeda, K. Domen, J. D. Epping, X. Fu, M. Antonietti, X. Wang, *Angew. Chem. Int. Ed. Engl.* **2010**, *49*, 441–444, *Angew. Chem.* **2010**, *122*, 451–454; m) J. Barrio, M. Volokh, M. Shalom, *J. Mater. Chem. A* **2020**, *8*, 11075–11116.
- [54] M. E. Lamanna, E. d I Horra, S. Jacobo, N. B. D'Accorso, *React. Funct. Polym.* **2009**, *69*, 759–765.
- [55] A. Savateev, S. Pronkin, J. D. Epping, M. G. Willinger, M. Antonietti, D. Dontsova, *J. Mater. Chem. A* **2017**, *5*, 8394–8401.
- [56] a) S. N. Talapaneni, G. Singh, I. Y. Kim, K. AlBahily, A. a H Al-Muhtaseb, A. S. Karakoti, E. Tavakkoli, A. Vinu, *Adv. Mater.* **2020**, *32*, 2070142; b) M. R. Benzigar, S. N. Talapaneni, S. Joseph, K. Ramadass, G. Singh, J. Scaranto, U. Ravon, K. Al-Bahily, A. Vinu, *Chem. Soc. Rev.* **2018**, *47*, 2680–2721.
- [57] G. P. Mane, S. N. Talapaneni, K. S. Lakhi, H. Ilbeygi, U. Ravon, K. Al-Bahily, T. Mori, D.-H. Park, A. Vinu, *Angew. Chem. Int. Ed. Engl.* **2017**, *56*, 8481–8485, *Angew. Chem.* **2017**, *129*, 8601–8605.
- [58] I. Y. Kim, S. Kim, S. Premkumar, J. H. Yang, S. Umapathy, A. Vinu, *Small* **2020**, *16*, 1903572.
- [59] a) W. Cha, I. Y. Kim, J. M. Lee, S. Kim, K. Ramadass, K. Gopalakrishnan, S. Premkumar, S. Umapathy, A. Vinu, *ACS Appl. Mater. Interfaces* **2019**, *11*, 27192–27199; b) T. Kesavan, T. Partheeban, M. Vivekanantha, N. Prabhu, M. Kundu, P. Selvarajan, S. Umapathy, A. Vinu, M. Sasiharan, *ACS Appl. Mater. Interfaces* **2020**, *12*, 24007–24018.
- [60] G. Zhang, M. Liu, T. Heil, S. Zafeiratos, A. Savateev, M. Antonietti, X. Wang, *Angew. Chem. Int. Ed. Engl.* **2019**, *58*, 14950–14954, *Angew. Chem.* **2019**, *131*, 15092–15096.
- [61] G. Zhang, L. Lin, G. Li, Y. Zhang, A. Savateev, S. Zafeiratos, X. Wang, M. Antonietti, *Angew. Chem. Int. Ed. Engl.* **2018**, *57*, 9372–9376, *Angew. Chem.* **2018**, *130*, 9516–9520.
- [62] X.-N. Cao, S. Lian, Y. Tong, W. Lin, L. Jia, Y. Fang, X. Wang, *Chem. Commun. (Camb.)* **2020**, *56*, 916–919.
- [63] P. Xia, S. Cao, B. Zhu, M. Liu, M. Shi, J. Yu, Y. Zhang, *Angew. Chem. Int. Ed. Engl.* **2020**, *59*, 5218–5225, *Angew. Chem.* **2020**, *132*, 5256–5263.
- [64] Y. Zou, J.-W. Shi, L. Sun, D. Ma, S. Mao, Y. Lv, Y. Cheng, *Chem. Eng. J.* **2019**, *378*, 122192.
- [65] Y. Zou, J.-W. Shi, D. Ma, Z. Fan, L. Cheng, D. Sun, Z. Wang, C. Niu, *ChemSusChem* **2018**, *11*, 1187–1197.
- [66] Y. Zou, J.-W. Shi, D. Ma, Z. Fan, C. He, L. Cheng, D. Sun, J. Li, Z. Wang, C. Niu, *Catal. Sci. Technol.* **2018**, *8*, 3883–3893.
- [67] a) H. Wang, L. Zhang, Z. Chen, J. Hu, S. Li, Z. Wang, J. Liu, X. Wang, *Chem. Soc. Rev.* **2014**, *43*, 5234–5244; b) S. Cao, J. Yu, *J. Phys. Chem. Lett.* **2014**, *5*, 2101–2107.
- [68] Y. Markushyna, C. A. Smith, A. Savateev, *Eur. J. Org. Chem.* **2019**, 1294–1309.
- [69] A. Savateev, M. Antonietti, *ChemCatChem* **2019**, *11*, 6166–6176.
- [70] A. Savateev, M. Antonietti, *ACS Catal.* **2018**, *8*, 9790–9808.
- [71] A. Savateev, I. Ghosh, B. König, M. Antonietti, *Angew. Chem. Int. Ed. Engl.* **2018**, *57*, 15936–15947, *Angew. Chem.* **2018**, *130*, 16164–16176.
- [72] a) Y. Zhang, N. Hatami, N. S. Lange, E. Ronge, W. Schilling, C. Jooss, S. Das, *Green Chem.* **2020**, *22*, 4516–4522; b) T. Niu, S. Chen, M. Hong, T. Zhang, J. Chen, X. Dong, B. Ni, *Green Chem.* **2020**, *22*, 5042–5049; c) Y.

- Dai, C. Li, Y. Shen, T. Lim, J. Xu, Y. Li, H. Niemantsverdriet, F. Besenbacher, N. Lock, R. Su, *Nat. Commun.* **2018**, *9*, 60.
- [73] a) M. Abdullah Khan, I. F. Teixeira, M. M. J. Li, Y. Koito, S. C. E. Tsang, *Chem. Commun. (Camb.)* **2016**, *52*, 2772–2775; b) Y. Zhao, M. Shalom, M. Antonietti, *Appl. Catal. B* **2017**, *207*, 311–315.
- [74] a) Q. Cao, B. Kumru, M. Antonietti, B. V. K. J. Schmidt, *Mater. Horiz.* **2020**, *7*, 762–786; b) P. Giusto, B. Kumru, J. Zhang, R. Rothe, M. Antonietti, *Chem. Mater.* **2020**, *32*, 7284–7291; c) N. Yandrapalli, T. Robinson, M. Antonietti, B. Kumru, *Small* **2020**, *16*, 2001180.
- [75] G. Wu, Y. Hu, Y. Liu, J. Zhao, X. Chen, V. Whoehling, C. Plesse, G. T. M. Nguyen, F. Vidal, W. Chen, *Nat. Commun.* **2015**, *6*, 7258.
- [76] a) P. Giusto, D. Cruz, T. Heil, H. Arazoe, P. Lova, T. Aida, D. Comoretto, M. Patrini, M. Antonietti, *Adv. Mater.* **2020**, *32*, 1908140; b) B. Kumru, V. Molinari, M. Shalom, M. Antonietti, B. V. K. J. Schmidt, *Soft Matter* **2018**, *14*, 2655–2664; c) B. Kumru, V. Molinari, M. Hilgart, F. Rummel, M. Schäffler, B. V. K. J. Schmidt, *Polym. Chem.* **2019**, *10*, 3647–3656; d) B. Kumru, M. Shalom, M. Antonietti, B. V. K. J. Schmidt, *Macromolecules* **2017**, *50*, 1862–1869.
- [77] M. H. S. Nathan, J. Gesmundo, J. Twilton, J. C. Tellis, D. W. C. MacMillan, D. A. Nicewicz, “Desk Reference and User’s Guide”, can be found under <https://www.sigmaaldrich.com/chemistry/chemical-synthesis/learning-center/photoredox-catalysis-guide.html>, **2020**.
- [78] C. K. Prier, D. A. Rankic, D. W. C. MacMillan, *Chem. Rev.* **2013**, *113*, 5322–5363.
- [79] N. A. Romero, D. A. Nicewicz, *Chem. Rev.* **2016**, *116*, 10075–10166.
- [80] Y. Yoshimi, M. Masuda, T. Mizunashi, K. Nishikawa, K. Maeda, N. Koshida, T. Itou, T. Morita, M. Hatanaka, *Org. Lett.* **2009**, *11*, 4652–4655.
- [81] K. Ohkubo, A. Fujimoto, S. Fukuzumi, *Chem. Commun. (Camb.)* **2011**, *47*, 8515–8517.
- [82] W. Yang, S. Yang, P. Li, L. Wang, *Chem. Commun. (Camb.)* **2015**, *51*, 7520–7523.
- [83] M. Rueping, S. Zhu, R. M. Koenigs, *Chem. Commun. (Camb.)* **2011**, *47*, 12709–12711.
- [84] M. H. Shaw, J. Twilton, D. W. C. MacMillan, *J. Org. Chem.* **2016**, *81*, 6898–6926.
- [85] a) G. Pandey, M. Karthikeyan, A. Murugan, *J. Org. Chem.* **1998**, *63*, 2867–2872; b) G. Pandey, R. Sochanchingwung, *J. Am. Chem. Soc.* **1994**, *116*, 1945–1946.
- [86] a) G. Pandey, R. Laha, *Angew. Chem. Int. Ed. Engl.* **2015**, *54*, 14875–14879; *Angew. Chem.* **2015**, *127*, 15088–15092; S. Hintz, J. Mattay, R. van Eldik, W.-F. Fu, *Eur. J. Org. Chem.* **1998**, 1583–1596.
- [87] A. J. Perkowski, C. L. Cruz, D. A. Nicewicz, *J. Am. Chem. Soc.* **2015**, *137*, 15684–15687.
- [88] H. Huang, Z. M. Strater, M. Rauch, J. Shee, T. J. Sisto, C. Nuckolls, T. H. Lambert, *Angew. Chem. Int. Ed. Engl.* **2019**, *58*, 13318–13322; *Angew. Chem.* **2019**, *131*, 13452–13456.
- [89] X. Wu, C. Meng, X. Yuan, X. Jia, X. Qian, J. Ye, *Chem. Commun. (Camb.)* **2015**, *51*, 11864–11867.
- [90] T. Keshari, V. K. Yadav, V. P. Srivastava, L. D. S. Yadav, *Green Chem.* **2014**, *16*, 3986–3992.
- [91] S. Cao, J. Low, J. Yu, M. Jaroniec, *Adv. Mater.* **2015**, *27*, 2150–2176.
- [92] a) C. Qiu, Y. Xu, X. Fan, D. Xu, R. Tandiana, X. Ling, Y. Jiang, C. Liu, L. Yu, W. Chen, C. Su, *Adv. Sci.* **2019**, *6*, 1801403; b) Z. Zhang, J. Huang, Q. Yuan, B. Dong, *Nanoscale* **2014**, *6*, 9250–9256; c) Z. Wu, H. Gao, S. Yan, Z. Zou, *Dalton Trans.* **2014**, *43*, 12013–12017.
- [93] A. Savateev, S. Pronkin, M. G. Willinger, M. Antonietti, D. Dontsova, *Chem. Asian J.* **2017**, *12*, 1517–1522.
- [94] a) B. Ni, B. Zhang, J. Han, B. Peng, Y. Shan, T. Niu, *Org. Lett.* **2020**, *22*, 670–674; b) Y. Cai, Y. Tang, L. Fan, Q. Lefebvre, H. Hou, M. Rueping, *ACS Catal.* **2018**, *8*, 9471–9476; c) Y. Zhao, M. Antonietti, *Angew. Chem. Int. Ed. Engl.* **2017**, *56*, 9336–9340; *Angew. Chem.* **2017**, *129*, 9464–9468; d) W.-J. Ong, L.-L. Tan, Y. H. Ng, S.-T. Yong, S.-P. Chai, *Chem. Rev.* **2016**, *116*, 7159–7329; e) J. Qin, S. Wang, H. Ren, Y. Hou, X. Wang, *Appl. Catal. B* **2015**, *179*, 1–8; f) M. Baar, S. Blechert, *Chem. Eur. J.* **2015**, *21*, 526–530; g) Y. Zheng, L. Lin, B. Wang, X. Wang, *Angew. Chem. Int. Ed. Engl.* **2015**, *54*, 12868–12884; *Angew. Chem.* **2015**, *127*, 13060–13077; h) Y. Wang, X. Wang, M. Antonietti, *Angew. Chem. Int. Ed. Engl.* **2012**, *51*, 68–89; *Angew. Chem.* **2012**, *124*, 70–92.
- [95] a) M. A. Bajada, A. Vijeta, A. Savateev, G. Zhang, D. Howe, E. Reisner, *ACS Appl. Mater. Interfaces* **2020**, *12*, 8176–8182; b) J. Khamrai, I. Ghosh, A. Savateev, M. Antonietti, B. König, *ACS Catal.* **2020**, *10*, 3526–3532; c) M. Woźnica, N. Chaoui, S. Taabache, S. Blechert, *Chem. Eur. J.* **2014**, *20*, 14624–14628; d) A. Vinu, K. Ariga, T. Mori, T. Nakanishi, S. Hishita, D. Golberg, Y. Bando, *Adv. Mater.* **2005**, *17*, 1648–1652; e) F. Su, S. C. Mathew, G. Lipner, X. Fu, M. Antonietti, S. Blechert, X. Wang, *J. Am. Chem. Soc.* **2010**, *132*, 16299–16301; f) I. Ghosh, J. Khamrai, A. Savateev, N. Shlapakov, M. Antonietti, B. König, *Science* **2019**, *365*, 360–366.
- [96] a) L. Lin, Z. Lin, J. Zhang, X. Cai, W. Lin, Z. Yu, X. Wang, *Nat. Can.* **2020**, *3*, 649–655; b) T. M. Suter, T. S. Miller, J. K. Cockcroft, A. E. Aliev, M. C. Wilding, A. Sella, F. Cora, C. A. Howard, P. F. McMillan, *Chem. Sci.* **2019**, *10*, 2519–2528; c) F. K. Kessler, W. Schnick, *Z. Anorg. Allg. Chem.* **2019**, *645*, 857–862; d) T. S. Miller, T. M. Suter, A. M. Telford, L. Picco, O. D. Payton, F. Russell-Pavier, P. L. Cullen, A. Sella, M. S. P. Shaffer, J. Nelson, V. Tileli, P. F. McMillan, C. A. Howard, *Nano Lett.* **2017**, *17*, 5891–5896; e) L. Lin, C. Wang, W. Ren, H. Ou, Y. Zhang, X. Wang, *Chem. Sci.* **2017**, *8*, 5506–5511; f) Y. Ham, K. Maeda, D. Cha, K. Takanae, K. Domen, *Chem. Asian J.* **2013**, *8*, 218–224; g) E. Wirnhier, M. Döblinger, D. Gunzelmann, J. Senker, B. V. Lotsch, W. Schnick, *Chem. Eur. J.* **2011**, *17*, 3213–3221; h) M. J. Bojdys, J. O. Muller, M. Antonietti, A. Thomas, *Chem. Eur. J.* **2008**, *14*, 8177–8182.
- [97] Z. Chen, S. Pronkin, T.-P. Fellingner, K. Kailasam, G. Vilé, D. Albani, F. Krumeich, R. Leary, J. Barnard, J. M. Thomas, J. Pérez-Ramírez, M. Antonietti, D. Dontsova, *ACS Nano* **2016**, *10*, 3166–3175.
- [98] H. Kasap, C. A. Caputo, B. C. M. Martindale, R. Godin, V. W.-h. Lau, B. V. Lotsch, J. R. Durrant, E. Reisner, *J. Am. Chem. Soc.* **2016**, *138*, 9183–9192.
- [99] a) S. Mazzanti, B. Kurpil, B. Pieber, M. Antonietti, A. Savateev, *Nat. Commun.* **2020**, *11*, 1387; b) A. Savateev, N. V. Tarakina, V. Strauss, T. Hussain, K. ten Brummelhuis, J. M. Sánchez Vadillo, Y. Markushyna, S. Mazzanti, A. P. Tyutyunnik, R. Walczak, M. Oschatz, D. M. Guldí, A. Karton, M. Antonietti, *Angew. Chem. Int. Ed. Engl.* **2020**, *59*, 15061–15068; *Angew. Chem.* **2020**, *132*, 15172–15180; c) Y. Markushyna, P. Lamagni, J. Catalano, N. Lock, G. Zhang, M. Antonietti, A. Savateev, *ACS Catal.* **2020**, *10*, 7336–7342; d) Y. Markushyna, C. Teutloff, B. Kurpil, D. Cruz, I. Laueremann, Y. Zhao, M. Antonietti, A. Savateev, *Appl. Catal. B* **2019**, *248*, 211–217; e) B. Kurpil, K. Otte, A. Mishchenko, P. Lamagni, W. Lipiński, N. Lock, M. Antonietti, A. Savateev, *Nat. Commun.* **2019**, *10*, 945; f) B. Kurpil, Y. Markushyna, A. Savateev, *ACS Catal.* **2019**, *9*, 1531–1538; g) Y. Markushyna, P. Lamagni, C. Teutloff, J. Catalano, N. Lock, G. Zhang, M. Antonietti, A. Savateev, *J. Mater. Chem. A* **2019**, *7*, 24771–24775; h) B. Kurpil, K. Otte, M. Antonietti, A. Savateev, *Appl. Catal. B* **2018**, *228*, 97–102; i) B. Kurpil, B. Kumru, T. Heil, M. Antonietti, A. Savateev, *Green Chem.* **2018**, *20*, 838–842; j) A. Savateev, B. Kurpil, A. Mishchenko, G. Zhang, M. Antonietti, *Chem. Sci.* **2018**, *9*, 3584–3591; k) A. Savateev, D. Dontsova, B. Kurpil, M. Antonietti, *J. Catal.* **2017**, *350*, 203–211; l) H. Schlöberg, J. Kröger, G. Savasci, M. W. Terban, S. Bette, I. Moudrakovski, V. Duppel, F. Podjaski, R. Siegel, J. Senker, R. E. Dinnebier, C. Ochsenfeld, B. V. Lotsch, *Chem. Mater.* **2019**, *31*, 7478–7486; m) F. Podjaski, J. Kröger, B. V. Lotsch, *Adv. Mater.* **2018**, *30*, 1705477; n) V. W.-h. Lau, D. Klose, H. Kasap, F. Podjaski, M.-C. Pignié, E. Reisner, G. Jeschke, B. V. Lotsch, *Angew. Chem. Int. Ed. Engl.* **2017**, *56*, 510–514; *Angew. Chem.* **2017**, *129*, 525–529; o) V. W.-h. Lau, I. Moudrakovski, T. Botari, S. Weinberger, M. B. Mesch, V. Duppel, J. Senker, V. Blum, B. V. Lotsch, *Nat. Commun.* **2016**, *7*, 12165.
- [100] Z. Chen, A. Savateev, S. Pronkin, V. Papaefthimiou, C. Wolff, M. G. Willinger, E. Willinger, D. Neher, M. Antonietti, D. Dontsova, *Adv. Mater.* **2017**, *29*, 1700555.
- [101] H. Ou, C. Tang, X. Chen, M. Zhou, X. Wang, *ACS Catal.* **2019**, *9*, 2949–2955.
- [102] G. Zhang, G. Li, Z.-A. Lan, L. Lin, A. Savateev, T. Heil, S. Zafeiratou, X. Wang, M. Antonietti, *Angew. Chem. Int. Ed. Engl.* **2017**, *56*, 13445–13449; *Angew. Chem.* **2017**, *129*, 13630–13634.
- [103] D. Dontsova, S. Pronkin, M. Wehle, Z. Chen, C. Fettkenhauer, G. Clavel, M. Antonietti, *Chem. Mater.* **2015**, *27*, 5170–5179.
- [104] a) L. Lin, H. Ou, Y. Zhang, X. Wang, *ACS Catal.* **2016**, *6*, 3921–3931; b) band positions and spectra of PTI are not presented for aforementioned reasons.
- [105] a) J. Albero, E. M. Barea, J. Xu, I. Mora-Seró, H. Garcia, M. Shalom, *Adv. Mater. Interfaces* **2017**, *4*, 1600265; b) H. Wang, S. Jiang, S. Chen, X. Zhang, W. Shao, X. Sun, Z. Zhao, Q. Zhang, Y. Luo, Y. Xie, *Chem. Sci.* **2017**, *8*, 4087–4092.
- [106] C. Merschjann, S. Tschierlei, T. Tyborski, K. Kailasam, S. Orthmann, D. Hollmann, T. Schedel-Niedrig, A. Thomas, S. Lochbrunner, *Adv. Mater.* **2015**, *27*, 7993–7999.
- [107] R. Godin, Y. Wang, M. A. Zwijnenburg, J. Tang, J. R. Durrant, *J. Am. Chem. Soc.* **2017**, *139*, 5216–5224.
- [108] a) H. Kisch, *Acc. Chem. Res.* **2017**, *50*, 1002–1010; b) H. Kisch, *Semiconductor Photocatalysis, Principles and Applications*, (Ed: H. Hennig), John Wiley & Sons, Weinheim **2015**; c) H. Kisch, *Angew. Chem. Int. Ed. Engl.* **2013**, *52*, 812–847; *Angew. Chem.* **2013**, *125*, 842–879.

- [109] A. Meyer, M. van Gastel, *J. Phys. Chem. A* **2011**, *115*, 1939–1945.
- [110] a) T. Hirakawa, P. V. Kamat, *J. Am. Chem. Soc.* **2005**, *127*, 3928–3934; b) P. V. Kamat, *J. Phys. Chem. Lett.* **2012**, *3*, 663–672; c) T. Hirakawa, P. V. Kamat, *Langmuir* **2004**, *20*, 5645–5647; d) X. Wang, T. Wu, H. Wang, X. Su, *Mater. Res. Bull.* **2016**, *73*, 423–428.
- [111] a) J. N. Schrauben, R. Hayoun, C. N. Valdez, M. Braten, L. Fridley, J. M. Mayer, *Science* **2012**, *336*, 1298–1301; b) T. Cai, Y. Liu, L. Wang, S. Zhang, J. Ma, W. Dong, Y. Zeng, J. Yuan, C. Liu, S. Luo, *ACS Appl. Mater. Interfaces* **2018**, *10*, 25350–25359; c) I. A. MacKenzie, L. Wang, N. P. R. Onuska, O. F. Williams, K. Begam, A. M. Moran, B. D. Dunietz, D. A. Nicewicz, *Nature* **2020**, *580*, 76–80.
- [112] J. W. Verhoeven, *Pure Appl. Chem.* **1996**, *68*, 2223–2286.
- [113] N. H. Damrauer, G. Cerullo, A. Yeh, T. R. Bousie, C. V. Shank, J. K. McCusker, *Science* **1997**, *275*, 54–57.
- [114] a) T. P. Yoon, M. A. Ischay, J. Du, *Nat. Chem.* **2010**, *2*, 527–532; b) T. Gensch, M. Teders, F. Glorius, *J. Org. Chem.* **2017**, *82*, 9154–9159.
- [115] a) H. Zhang, A. Yu, *J. Phys. Chem. C* **2014**, *118*, 11628–11635; b) Xu, M. Shalom, *ChemPhotoChem* **2019**, *3*, 170–179; c) J. Xu, M. Shalom, F. Piersimoni, M. Antonietti, D. Neher, T. J. K. Brenner, *Adv. Opt. Mater.* **2015**, *3*, 913–917; d) Q. Cui, J. Xu, X. Wang, L. Li, M. Antonietti, M. Shalom, *Angew. Chem. Int. Ed. Engl.* **2016**, *55*, 3672–3676, *Angew. Chem.* **2016**, *128*, 3736–3740.
- [116] J. Han, H. Y. Zou, M. X. Gao, C. Z. Huang, *Talanta* **2016**, *148*, 279–284.
- [117] H. Wang, S. Jiang, S. Chen, D. Li, X. Zhang, W. Shao, X. Sun, J. Xie, Z. Zhao, Q. Zhang, Y. Tian, Y. Xie, *Adv. Mater.* **2016**, *28*, 6940–6945.
- [118] M. B. Plutschack, B. Pieber, K. Gilmore, P. H. Seeberger, *Chem. Rev.* **2017**, *117*, 11796–11893.
- [119] C. G. Thomson, A.-L. Lee, F. Vilela, *Beilstein J. Org. Chem.* **2020**, *16*, 1495–1549.
- [120] a) C. Sambiagio, T. Noël, *Trends Chem.* **2020**, *2*, 92–106; b) G. Vilé, S. Richard-Bildstein, A. Lhuillery, G. Rueedi, *ChemCatChem* **2018**, *10*, 3786–3794; c) G. Laudadio, Y. Deng, K. van der Wal, D. Ravelli, M. Nuño, M. Fagnoni, D. Guthrie, Y. Sun, T. Noël, *Science* **2020**, *369*, 92–96; d) L. Amini-Rentsch, E. Vanoli, S. Richard-Bildstein, R. Marti, G. Vilé, *Ind. Eng. Chem. Res.* **2019**, *58*, 10164–10171.
- [121] a) J. P. Barham, E. Koyama, Y. Norikane, N. Ohneda, T. Yoshimura, *Chem. Rec.* **2019**, *19*, 188–203; b) J. P. Barham, S. Tamaoki, H. Egami, N. Ohneda, T. Okamoto, H. Odajima, Y. Hamashima, *Org. Biomol. Chem.* **2018**, *16*, 7568–7573; c) E. Koyama, N. Ito, J.-i. Sugiyama, J. P. Barham, Y. Norikane, R. Azumi, N. Ohneda, Y. Ohno, T. Yoshimura, H. Odajima, T. Okamoto, *J. Flow Chem.* **2018**, *8*, 147–156; d) J. P. Barham, S. Tanaka, E. Koyama, N. Ohneda, T. Okamoto, H. Odajima, J.-i. Sugiyama, Y. Norikane, *J. Org. Chem.* **2018**, *83*, 4348–4354; e) S. Tortoioli, A. Friedli, A. Prud'homme, S. Richard-Bildstein, P. Kohler, S. Abele, G. Vilé, *Green Chem.* **2020**, *22*, 3748–3758.
- [122] T. Noël in *Photochemical Processes in Continuous-Flow Reactors*, World Scientific, London, **2017**, ch.9 pp. 245–267.
- [123] K. C. Harper, E. G. Moschetta, S. V. Bordawekar, S. J. Wittenberger, *ACS Cent. Sci.* **2019**, *5*, 109–115.
- [124] D. Cambié, C. Bottecchia, N. J. W. Straathof, V. Hessel, T. Noël, *Chem. Rev.* **2016**, *116*, 10276–10341.
- [125] J. J. Douglas, M. J. Sevrin, C. R. J. Stephenson, *Org. Process Res. Dev.* **2016**, *20*, 1134–1147.
- [126] A. K. Gaigalas, H.-J. He, L. Wang, *J. Res. Natl. Inst. Stand. Technol.* **2009**, *114*, 69–81.
- [127] A. Ufer, D. Sudhoff, A. Mescher, D. W. Agar, *Chem. Eng. J.* **2011**, *167*, 468–474.
- [128] C. Yang, R. Li, K. A. I. Zhang, W. Lin, K. Landfester, X. Wang, *Nat. Commun.* **2020**, *11*, 1239.
- [129] B. Pieber, M. Shalom, M. Antonietti, P. H. Seeberger, K. Gilmore, *Angew. Chem. Int. Ed. Engl.* **2018**, *57*, 9976–9979, *Angew. Chem.* **2018**, *130*, 10127–10131.
- [130] I. Krivtsov, D. Mitoraj, C. Adler, M. Ilkaeva, M. Sardo, L. Mafrá, C. Neumann, A. Turchanin, C. Li, B. Dietzek, R. Leiter, J. Biskupek, U. Kaiser, C. Im, B. Kirchhoff, T. Jacob, R. Beranek, *Angew. Chem. Int. Ed. Engl.* **2020**, *59*, 487–495, *Angew. Chem.* **2020**, *132*, 495–503.
- [131] C. Rosso, S. Gisbertz, J. D. Williams, H. P. L. Gemoets, W. Debrouwer, B. Pieber, C. O. Kappe, *React. Chem. Eng.* **2020**, *5*, 597–604.
- [132] O. Levenspiel, in *Chemical Reaction Engineering*, 3rd ed., John Wiley & Sons, **1998**, pp. 120.
- [133] a) C. D. Mboyi, C. Testa, S. Reeb, S. Genc, H. Cattey, P. Fleurat-Lessard, J. Roger, J.-C. Hierso, *ACS Catal.* **2017**, *7*, 8493–8501; b) F. Allouch, N. V. Vologdin, H. Cattey, N. Pirio, D. Naoufal, A. Kanj, R. V. Smaliy, A. Savateev, A. Marchenko, A. Hurieva, H. Koidan, A. N. Kostyuk, J.-C. Hierso, *J. Organomet. Chem.* **2013**, *735*, 38–46.
- [134] X. Hu, *Chem. Sci.* **2011**, *2*, 1867–1886.
- [135] C. M. Lavoie, M. Stradiotto, *ACS Catal.* **2018**, *8*, 7228–7250.
- [136] J. A. Milligan, J. P. Phelan, S. O. Badir, G. A. Molander, *Angew. Chem. Int. Ed. Engl.* **2019**, *58*, 6152–6163, *Angew. Chem.* **2019**, *131*, 6212–6224.
- [137] a) C. Zhu, H. Yue, L. Chu, M. Rueping, *Chem. Sci.* **2020**, *11*, 4051–4064; b) J. C. Tellis, D. N. Primer, G. A. Molander, *Science* **2014**, *345*, 433–436.
- [138] Z. Zuo, D. T. Ahneman, L. Chu, J. A. Terrett, A. G. Doyle, D. W. C. MacMillan, *Science* **2014**, *345*, 437–440.
- [139] A. Vijeta, E. Reisner, *Chem. Commun. (Camb.)* **2019**, *55*, 14007–14010.
- [140] B. Pieber, J. A. Malik, C. Cavedon, S. Gisbertz, A. Savateev, D. Cruz, T. Heil, G. Zhang, P. H. Seeberger, *Angew. Chem. Int. Ed. Engl.* **2019**, *58*, 9575–9580, *Angew. Chem.* **2019**, *131*, 9676–9681.
- [141] C. Cavedon, A. Madani, P. H. Seeberger, B. Pieber, *Org. Lett.* **2019**, *21*, 5331–5334.
- [142] Y. Qin, B. C. M. Martindale, R. Sun, A. J. Rieth, D. G. Nocera, *Chem. Sci.* **2020**, *11*, 7456–7461.
- [143] S. Gisbertz, S. Reischauer, B. Pieber, *Nat. Can.* **2020**, *3*, 611–620.
- [144] H. Wang, S. Jin, X. Zhang, Y. Xie, *Angew. Chem. Int. Ed. Engl.* **2020**, DOI 10.1002/anie.202002241.

Manuscript received: August 31, 2020  
Revised manuscript received: November 4, 2020  
Accepted manuscript online: November 5, 2020